Available online at www.sciencedirect.com
ScienceDirect
Gondwana Research 10 (2006) 277–300
www.elsevier.com/locate/gr

Zircon geochronology and Sm–Nd isotopic study: Further constraints for the Archean and Paleoproterozoic geodynamical evolution of the southeastern Guiana Shield, north of Amazonian Craton, Brazil

Lúcia T. da Rosa-Costa [a,*], Jean M. Lafon [b], Claude Delor [c]

[a] *CPRM-Geological Survey of Brazil, Belém, Brazil*
[b] *Pará-Iso Laboratory, Universidade Federal do Pará, Belém, Brazil*
[c] *BRGM-Geological Survey of France, Orléans, France*

Received 27 June 2005; accepted 24 February 2006
Available online 7 September 2006

Abstract

The eastern part of the Guiana Shield, northern Amazonian Craton, in South America, represents a large orogenic belt developed during the Transamazonian orogenic cycle (2.26–1.95 Ga), which consists of extensive areas of Paleoproterozoic crust and two major Archean terranes: the Imataca Block, in Venezuela, and the here defined Amapá Block, in the north of Brazil.

Pb-evaporation on zircon and Sm–Nd on whole rock dating were provided on magmatic and metamorphic units from southwestern Amapá Block, in the Jari Domain, defining its long-lived evolution, marked by several stages of crustal accretion and crustal reworking. Magmatic activity occurred mainly at the Meso-Neoarchean transition (2.80–2.79 Ga) and during the Neoarchean (2.66–2.60 Ga). The main period of crust formation occurred during a protracted episode at the end of Paleoarchean and along the whole Mesoarchean (3.26–2.83 Ga). Conversely, crustal reworking processes have dominated in Neoarchean times. During the Transamazonian orogenic cycle, the main geodynamic processes were related to reworking of older Archean crust, with minor juvenile accretion at about 2.3 Ga, during an early orogenic phase. Transamazonian magmatism consisted of syn- to late-orogenic granitic pulses, which were dated at 2.22 Ga, 2.18 Ga and 2.05–2.03 Ga. Most of the ε_{Nd} values and T_{DM} model ages (2.52–2.45 Ga) indicate an origin of the Paleoproterozoic granites by mixing of juvenile Paleoproterozoic magmas with Archean components.

The Archean Amapá Block is limited in at southwest by the Carecuru Domain, a granitoid-greenstone terrane that had a geodynamic evolution mainly during the Paleoproterozoic, related to the Transamazonian orogenic cycle. In this latter domain, a widespread calc-alkaline magmatism occurred at 2.19–2.18 Ga and at 2.15–2.14 Ga, and granitic magmatism was dated at 2.10 Ga. Crustal accretion was recognized at about 2.28 Ga, in agreement with the predominantly Rhyacian crust-forming pattern of the eastern Guiana Shield. Nevertheless, T_{DM} model ages (2.50–2.38 Ga), preferentially interpreted as mixed ages, and $\varepsilon_{Nd} < 0$, point to some participation of Archean components in the source of the Paleoproterozoic rocks. In addition, the Carecuru Domain contains an oval-shaped Archean granulitic nucleus, named Paru Domain. In this domain, Neoarchean magmatism at about 2.60 Ga was produced by reworking of Mesoarchean crust, as registered in the Amapá Block. Crustal accretion events and calc-alkaline magmatism are recognized at 2.32 Ga and at 2.15 Ga, respectively, as well as charnockitic magmatism at 2.07 Ga.

The lithological association and the available isotopic data registered in the Carecuru Domain suggests a geodynamic evolution model based on the development of a magmatic arc system during the Transamazonian orogenic cycle, which was accreted to the southwestern border of the Archean Amapá Block.

Keywords: Archean; Paleoproterozoic; Transamazonian orogenesis; Crustal evolution; Amazonian Craton

1. Introduction

The Guiana Shield represents the northern segment of the Amazonian Craton, in South America, located on the northern edge of the Amazon Basin (Fig. 1). With an area of nearly

* Corresponding author. Postal address: Companhia de Pesquisa de Recursos Minerais, Avenida Dr. Freitas, 3645, Bairro do Marco, CEP 66095-110, Belém, Pará, Brazil.
E-mail address: ltravassos@amazon.com.br (L.T. da Rosa-Costa).

1342-937X/$ - see front matter
doi:10.1016/j.gr.2006.02.012

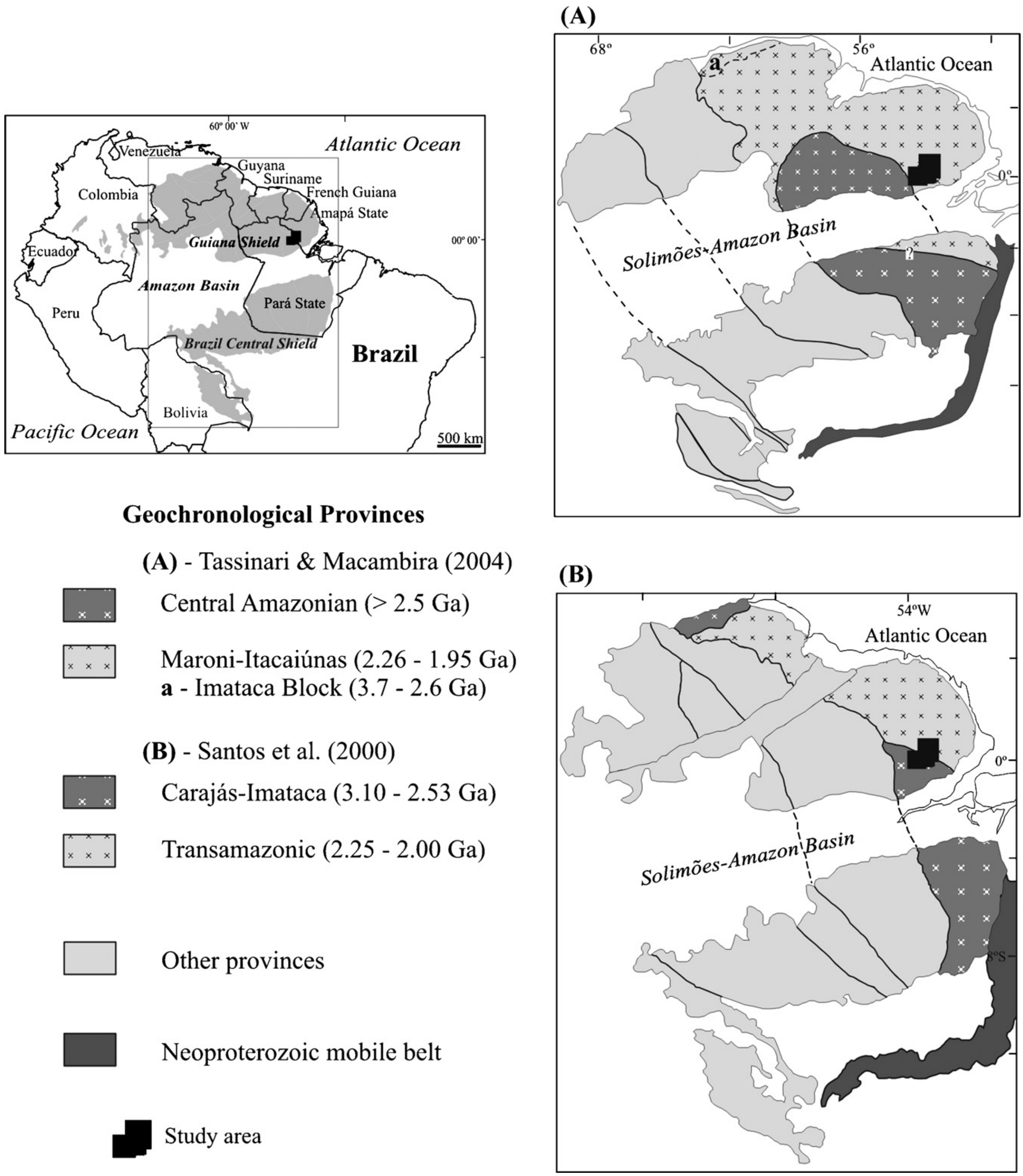

Fig. 1. Location map and simplified sketch maps of the Amazonian Craton showing geochronological provinces according to proposals of (A) Tassinari and Macambira (2004) and (B) Santos et al. (2000).

1.5 million km^2, it is one of the major Precambrian segments of the Western Gondwana. The eastern portion of the Guiana Shield consists of an exceptionally large Paleoproterozoic belt, exceeding 1200 km in length and 400 km in width, making it one of the largest Paleoproterozoic domains in the world. This belt extends from northern Brazil to eastern Venezuela, including French Guiana, Suriname and Guyana, and matches with the Eburnean orogen in the West Africa Craton (Onstott and Hargraves, 1981; Onstott et al., 1984; Ledru et al., 1994; Zhao et al., 2002).

The geochronological pattern of this belt indicates that its evolution took place during the Transamazonian orogenic cycle (2.26–1.95 Ga), mainly in Rhyacian times (Gruau et al., 1985;

Teixeira et al., 1989; Sato and Tassinari, 1997; Vanderhaeghe et al., 1998; Lafrance et al., 1999; Nogueira et al., 2000; Norcross et al., 2000; Tassinari et al., 2000; Voicu et al., 2000; Avelar, 2002; Avelar et al., 2003; Delor et al., 2003a,b; Roever et al., 2003). It consists mostly of gneissic-migmatitic-granulitic complexes, greenstone belts and granitoids, with variable chemical and structural features, defining several evolutionary episodes of juvenile crustal accretion, followed by crustal reworking. However, Archean remnants have been recognized, principally in eastern Venezuela (Montgomery and Hurley, 1978; Montgomery, 1979; Tassinari et al., 2001, 2004) and in some sectors of northwest Pará and centre–southwest Amapá states, in Brazil (João and Marinho, 1982; Lima et al., 1982; Montalvão and Tassinari, 1984; Lafon et al., 1998; Ricci et al., 2002; Avelar et al., 2003; Rosa-Costa et al., 2001, 2003; Klein et al., 2003; Faraco et al., 2004).

This Transamazonian orogen corresponds to a remarkable geochronological province of the Amazonian Craton, named Maroni-Itacaiúnas (Cordani et al., 1979; Tassinari and Macambira, 2004) or Transamazonic (Santos et al., 2000), which was accreted to an Archean province unaffected by post-Archean orogens, the Central Amazonian or Carajás Province (Fig. 1A and B).

Despite the difficulties of field access, due to dense rain forest and thick soil cover developed over the Precambrian substratum, the geological knowledge of this Paleoproterozoic belt has considerably been improved in recent years. Especially in French Guiana, where preserved Archean rocks are unknown, detailed mapping and geochronological program led to the understanding of the geodynamic evolution of juvenile domains during Transamazonian orogenic cycle (Vanderhaeghe et al., 1998; Delor et al., 2003a,b).

However, concerning to more ensialic domains, even if Archean protoliths have been broadly recognized, as cited above, the nature, the geographical extension of the Archean segments and their relationships with Paleoproterozoic domains remain poorly understood. In addition, the occurrence of reworked Archean crust has promoted an extensive debate concerning to the location of the boundary between the Archean and Paleoproterozoic geochronological provinces of the eastern Amazonian Craton.

In NW Pará and SW Amapá states, geological mapping carried out by CPRM-Geological Survey of Brazil (see Carvalho et al., 2001; Ricci et al., 2001) led to the recognition of juxtaposed geological domains, which present distinct lithological content, metamorphic history, geophysical and structural signatures (Ricci et al., 2001). Recent Pb–Pb and Sm–Nd dating indicated that these domains present, individually, dominating Archean or dominating Paleoproterozoic geochronological patterns (Pimentel et al., 2002; Ricci et al., 2002; Avelar et al., 2003; Rosa-Costa et al., 2001, 2003; Klein et al., 2003; Faraco et al., 2004).

This study is focused on the western portion of the area recently mapped by CPRM, where the Jari, Carecuru and Paru Domains have been defined. An expressive group of single zircon Pb-evaporation ages and Sm–Nd T_{DM} model ages, acquired on igneous and metaigneous rocks from the different domains are presented, in order to identify the main crustal growth episodes and magmatic events in each domain and to discuss the main geodynamic processes responsible for the present-day configuration of the distinct domains, in the context of the major geochronological provinces of the Amazonian Craton.

2. Precambrian geological setting and previous geochronology

The tectonic models that have been proposed for the Amazonian Craton conceive the partitioning of this craton into large geochronological provinces that have distinctive ages, structural patterns and geodynamic evolution. In the current literature, two models prevail and are displayed in Fig. 1. The first one has been initially proposed by Cordani et al. (1979) and then refined by many authors (Teixeira et al., 1989; Sato and Tassinari, 1997; Tassinari and Macambira, 1999; Tassinari et al., 2000; Tassinari and Macambira, 2004), while the other was proposed by Santos et al. (2000).

The boundaries between provinces have been supported mainly by geochronological data. However, some of these limits are still under discussion, due to the lack of reliable geological and geochronological information. Concerning to the northeastern portion of the craton, which coincides approximately with the eastern part of the Guiana Shield, the debate is focused on the extension of preserved or reworked Archean crust in the Paleoproterozoic domains.

According to the proposition of Tassinari and Macambira (2004), the eastern part of the Guiana Shield is included in the Maroni-Itacaiúnas Province, a widespread Paleoproterozoic belt accreted to an Archean block (the Central Amazonian Province) during the Transamazonian orogenic cycle. This province was defined as constituted of large areas of Paleproterozoic crust, incorporating some remnants of an older Archean basement, such as the expressive allochthonous Imataca Block (3.7–2.6 Ga) in Venezuela (Montgomery and Hurley, 1978; Montgomery, 1979; Tassinari et al., 2001, 2004), or the restricted inliers that occur in Amapá state (Cupixi region–Montalvão and Tassinari, 1984; Sato and Tassinari, 1997–and Tartarugalzinho region–João and Marinho, 1982; Lima et al., 1982; Lafon et al., 1998). The southern limit of the Maroni-Itacaiúnas Province with the Central Amazonian Province was positioned at the north of the Archean Carajás range, in central Brazil Shield (Cordani et al., 1984).

The Transamazonic Province of Santos et al. (2000) roughly corresponds to the Maroni-Itacaiúnas Province. However, these authors excluded the Imataca Complex of the province and extended the Archean Carajás Province up to the southeastern most portion of Guiana Shield (Fig. 1), incorporating the Archean inlier of the Cupixi region, in the Amapá state.

In French Guiana, a geodynamical model has been proposed by Vanderhaeghe et al. (1998), and refined by Delor et al. (2003a,b), to account for the Transamazonian evolution of juvenile sectors of the Paleoproterozoic belt. Vanderhaeghe et al. (1998) proposed a two-stage model, which follows the formation of an oceanic crust at 2.17 Ga. The first stage is related to crustal growth by magmatic accretion in a magmatic arc context, defined by calc-alkaline plutonism and greenstone belt formation between 2.14 and 2.11 Ga. The second stage is marked by crustal recycling and tectonic accretion, during oblique convergence between juvenile blocks, which was responsible for the formation of pull-apart basins and for the emplacement of high-K granites at 2.09–2.08 Ga.

According to Delor et al. (2003a), the earlier stage consists of the formation of juvenile oceanic crust between 2.26 and 2.20 Ga, followed by a stage of dominant TTG magmatism and development of greenstone belt sequences, between 2.18 and 2.13 Ga, in a scenario of island-arc, in response to a mainly southward-directed subduction. Granitic magmatism and migmatization of earlier TTG-greenstone sequences occurred between 2.11 and 2.08 Ga due to the closure of island-arc basins. Formation of pull-apart basins is also associated to this stage. A further stage of oblique plate convergence, at 2.07–2.06 Ga, is marked by the production of metaluminous granites emplaced along strike-slip shear zones. These authors consider this stage synchronous with the metamorphic climax of the ultrahigh temperature (UHT) metamorphic event of the Bakhuis granulites, in Suriname (Delor et al., 2003b; Roever et al., 2003), which is also suspected in central and northern Amapá (Avelar et al., 2001; Lafon et al., 2001).

In face of the juvenile nature of the domains of the eastern part of Guiana Shield, in recent years, Archean protoliths, dated between 3.3 and 2.6 Ga, have extensively been documented in its southeastern most portion (Pimentel et al., 2002; Ricci et al., 2002; Avelar et al., 2003; Klein et al., 2003; Rosa-Costa et al., 2003; Faraco et al., 2004). In this region, Archean records occur mainly between the border of Pará and Amapá states and the Tartarugal region (central of Amapá state), defining a more ensialic nature to this section of the Transamazonian orogen.

Field observations, together with map interpretations and petrographic studies, led Ricci et al. (2001) to propose a tectonic partitioning of the NW Pará and SW Amapá region into distinct tectonic domains, bounded by first-order strike-slip shear zones, named from northeast to southwest, Cupixi-Tartarugal Grande Ancient Terrane, Jari Belt and Carecuru-Paru Orogen (Fig. 2). These authors recognized that each domain has distinct lithological content, metamorphic history, geophysical and structural signatures, representing tectonostratigraphic terranes, sensu Howell (1995).

Rosa-Costa et al. (2003) renamed these terranes simply as "domains" and presented a new set of single zircon Pb-evaporation ages, which combined with previous published data (Montalvão and Tassinari, 1984; Sato and Tassinari, 1997; Pimentel et al., 2002; Ricci et al., 2002; Avelar et al., 2003), indicate a dominant Archean age pattern for the Cupixi and Jari Domains, whereas the Carecuru Domain presents a dominant Paleoproterozoic age pattern. The latter includes an oval-shaped domain, named Paru, which also contains Archean rocks.

This study is focused on the Jari, Carecuru and Paru Domains, corresponding to the centre–southwest portion of the area studied by Ricci et al. (2001). The main lithological units of these domains can be observed in Fig. 2, as well as the available geochronological records.

The Jari Domain is a linear range, approximately 100 km wide, extending over the eastern boundary of the investigated area, interposed between the Cupixi and Carecuru Domains. The Jari Domain is characterized by a conspicuous NW–SE ductile structuring, constituted mainly of high-grade rocks that are represented by the granulitic orthogneisses of the Jari-Guaribas Complex (enderbitic and charnockitic banded gneisses, with layers or enclaves of massive to foliated mafic granulites), mesoperthite and/or clinopyroxene-bearing granitic orthogneisses of the amphibolite-granulite transition facies included in the Baixo Mapari Complex, and catazonal granites grouped in the Noucouru Intrusive Suite (charnockites, enderbites and mesoperthite-bearing granites). Minor high-grade metasedimentary rocks occur as narrow belts, surrounded by orthogneisses, defining the Iratapuru Complex (aluminous gneisses, garnet and sillimatite-bearing quartzites, clinopyroxene-bearing BIFs, kinzigites and khondalites). Amphibolite-facies grey gneisses (mainly tonalitic and granodioritic gneisses) of the Guianense Complex are also included in the basement of the Jari Domain. High- to medium-grade gneisses that can not be inserted in specific stratigraphic units, complement the basement assemblage of the Jari Domain, and are informally referred to as granulitic-gneissic-migmatitic complex. All the metamorphic complexes are heterogeneously affected by migmatization and locally retrograded to amphibolite and greenschist facies metamorphism.

Neoarchean Pb–Pb zircon ages were obtained on enderbitic gneiss of the Jari-Guaribas Complex and on granodioritc gneiss of the Guianense Complex (respectively 2797±3 Ma and 2652±4 Ma, Rosa-Costa et al., 2003) and on igneous charnoenderbite of the Noucouru Intrusive Suite (2605±6 Ma—Ricci et al., 2002). In addition, a tonalitic gneiss of the Guianense Complex, yielded a Paleoarchean Pb–Pb zircon age (3321±11 Ma—Klein et al., 2003).

The Carecuru Domain represents a Paleoproterozoic granitoid-greenstone domain. The plutonic assemblage is constituted mainly of diorites and tonalites, with minor granodiorites, composing a lithological association consistent with the calc-alkaline series (e.g. Lameyre and Bowden, 1982; Barbarin, 1990). These rocks are heterogeneously deformed, showing strongly penetrative foliation to preserved igneous texture, and are included in the Paru-Maratiá Complex, dated at 2150±1 Ma, and in the Carecuru Intrusive Suite, dated at 2140±1 Ma (Rosa-Costa et al., 2003). Concerning to the supracrustal sequences, the most expressive is the Ipitinga Group, which marks the boundary between the Jari and Carecuru Domains. This group is composed of mafic–ultramafic metavolcanic schists, BIFs, metasedimentary schists and quartzites, metamorphosed under greenschist and amphibolite facies. Sm–Nd isochronic age dates this sequence at about 2264±34 Ma (McReath and Faraco, 1997). Minor undated supracrustal sequences (Fazendinha, 13 de Maio and Cuiapocu sequences), composed principally of mafic- to intermediated metavolcanics, occur as discontinuous strips, overlaying the plutonic units.

The Paru Domain represents an inlier within the Carecuru Domain, composed mainly of Neoarchean (2597±4 Ma—Rosa-Costa et al., 2003) granulitic orthogneisses of the Ananaí Complex (enderbitic and charnoenderbitic gneisses, with minor mafic granulites) and Paleoproterozoic (2.16–2.06 Ga) intrusive charnockites and mesoperthite-granites, grouped in the Igarapé Urucu Intrusive Suite.

Plutons of granitoids with variable compositional and structural characteristics are widespread in all domains. They cross-cut metamorphic complexes or supracrustal sequences

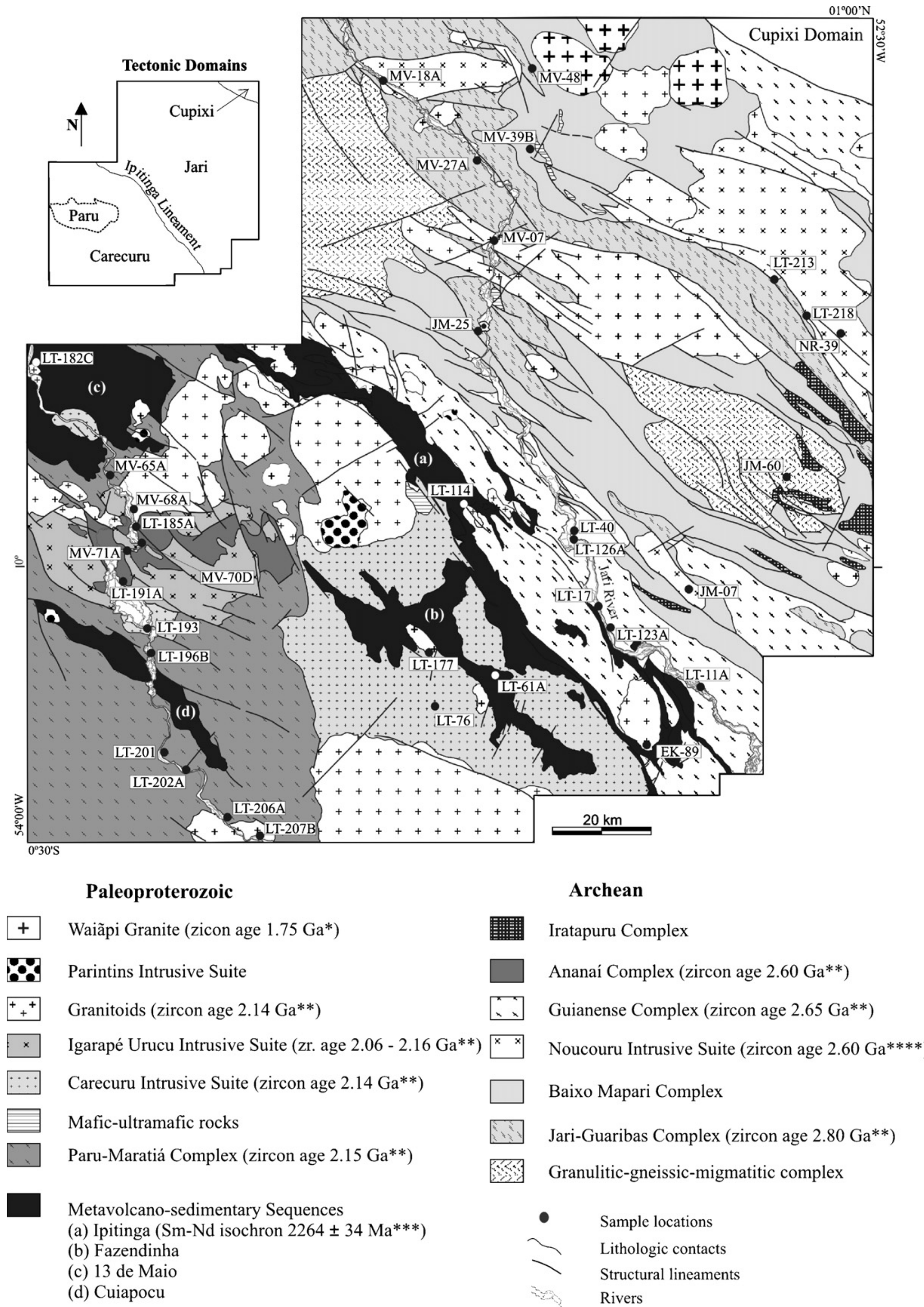

Fig. 2. Geological map of the study area, showing the sites of the samples dated in this work. Geological map, stratigraphic arrange and tectonic subdivision (sketch on top-left) are based on Carvalho et al. (2001) and Ricci et al. (2001). Previous geochronological data compiled from: Vasquez and Lafon (2001)*, Rosa-Costa et al. (2003)**, McReath and Faraco (1997)*** and Ricci et al. (2002)****.

and represent different magmatic episodes of the Transamazonian orogenic cycle. The Parintins Intrusive Suite groups the late- to post-orogenic granitoids, composed mainly of granites and granodiorites, massive or weakly deformed. Moreover, several plutons, composed mainly by leucogranites, with minor granodiorites and tonalites are widespread. Due to the lack of conclusive geological information, they are informally referred as Granitoids. Preliminary Pb–Pb zircon dating of these plutons, registered a magmatic pulse at 2146±3 Ma in the Jari Domain (Rosa-Costa et al., 2003).

Post-Transamazonian rocks are scarce in the investigated area, being restricted to three roughly circular plutons of A-type granites, referred as Waiãpi Granite, dated at 1753±3 Ma (Vasquez and Lafon, 2001).

3. Geochronological study

3.1. Sampling and experimental procedure

Geochronological investigations were carried out on gneisses, granitoids and metavolcanic rocks, which represent the key lithologic units of the Jari, Carecuru and Paru Domains. The samples selected for the geochronological study were taken away from veins, migmatitic segregation and lithologic contacts, in order to avoid contamination. The sample locations are shown in Fig. 2. The geographic coordinates and brief sample descriptions are presented in Appendix A.

The geochronological study was based on zircon Pb-evaporation (Kober, 1986, 1987) and whole rock Sm–Nd methods. All the isotopic analyses were carried out with a Finnigan MAT262 mass spectrometer at the Laboratório de Geologia Isotópica (Pará-Iso) of the Universidade Federal do Pará (UFPA), Belém, Brazil. Sample preparation was done at laboratories of CPRM-Geological Survey of Brazil and UFPA.

Zircon crystals were dated using double Re filaments, and the isotopic data were acquired in the dynamic mode, using an ion-counting system. The Pb isotope compositions were determined through repeated analyses of several zircon grains from the sample, at increasing evaporation temperature steps. The $^{207}Pb/^{206}Pb$ ratios were corrected from mass discrimination using a factor of 0.12%±0.03 per u.m.a., determined by repeated analyses of the NBS-982 "equal atoms" Pb standard. The calculation of common lead correction was done using the Pb composition of the Stacey and Kramers (1975) model, at the age of the grain. Analyses with $^{206}Pb/^{204}Pb$ ratios lower than 2500 were eliminated to minimize the effects of common lead correction on the radiogenic isotopic ratios and they are not shown in the tables of data.

The Pb-evaporation method usually provides very precise measurements of the $^{207}Pb/^{206}Pb$ ratio, which enable the determination of a precise weighted average value for the age (±1–5 Ma) on a small number of grains. As Pb/U ratios are not determined, the oldest $^{207}Pb/^{206}Pb$ age is a minimum age. However, the assumption that this age can represent a "concordant" crystallization age of zircon from magmatic rocks is strongly supported when repeated measurements of $^{207}Pb/^{206}Pb$ do not vary significantly in several crystals and at different temperature steps in one grain (Kober et al., 1989; Ansdell and Kyser, 1993; Karabinos and Gromet, 1993; Kröner et al., 1999).

The age of each sample is calculated using the mean value of the $^{207}Pb/^{206}Pb$ ratios at the highest temperature steps. When different temperature steps of the same grain furnish similar ages, all of them are included in the mean age calculation of this grain. Consequently, the confidence of the result depends on the number of grains with similar ages and, at least three grains with similar ages are necessary to define a crystallization age. Grains furnishing ages significantly lower are suspected to have suffered lead loss after crystallization and are arbitrarily discarded. In the same way, grains yielding isolated older ages are considered as inherited and, consequently, are also arbitrarily discarded. The weighted mean and the 2σm errors on the age of the remaining zircon population were calculated following Gaudette et al. (1998). An age calculation using the Ludwig's 2000 Isoplot program would furnish statistically indistinguishable results as discussed in Delor et al. (2003a). Pb-evaporation age diagrams were drawn using the Isoplot program (Ludwig, 2004).

The chemical procedures for sample dissolution and Sm and Nd extraction have previously been described in Klein et al. (2005). The rock powders (~100 mg) were dissolved with a mixture of HF $+HNO_3$ in Teflon vessels at 220 °C. REE were separated from the other elements by cation exchange chromatography using a Biorad Dowex 50×8 resin in HCl and HNO_3 media. Then, Sm and Nd were separated from the REE by anion exchange chromatography on Biorad Dowex AG1×4 in HNO_3–methanol medium. A mixed ^{150}Nd–^{149}Sm spike was introduced for determination of Sm and Nd concentrations. The isotopic measurements of Sm and Nd were performed in multi-collection static mode, using a Ta–Re double filament. The mean $^{143}Nd/^{144}Nd$ value obtained during the study on repeated analyses of the La Jolla Standard was 0.511834±18 (2σ) and the Nd data were normalized to a $^{143}Nd/^{144}Nd$ ratio of 0.7219. The total blanks do not exceed 0.24 ng for Sm and 0.61 ng for Nd. Nd model ages for all the samples were calculated using the DePaolo (1981) model for a depleted mantle evolution (T_{DM}), excluding those with $^{147}Sm/^{144}Nd$ outside the range of 0.088–0.125, since a "single stage" Sm/Nd evolution is doubtful for the Sm/Nd system of these samples.

3.2. Isotopic results and discussion

3.2.1. Zircon ages — constraining the magmatic events

Zircon populations from 16 rock samples have been investigated. The results are shown in Table 1, and organized according to their original domain and stratigraphic unit they belong to. Pb-evaporation diagrams of the dated samples are shown in Figs. 3 and 4.

3.2.1.1. Jari Domain. Two samples of enderbitic gneisses (JM-60 and MV-27A) from the Jari-Guaribas Complex were investigated in order to determine the age of the igneous precursor of the granulites. In sample JM-60, two distinct zircon populations were individualized: one defined by elongated and sub-euhedral grains and the other by rounded crystals. Nevertheless, both populations exhibit contrasted fine zoning, as

Table 1
Zircon Pb-evaporation isotopic results for the dated samples

Zircon grain	T (°C)	No. of ratios	$^{206}Pb/^{204}Pb$	$^{208}Pb/^{206}Pb$	2σ	$^{207}Pb/^{206}Pb$	$^{207}Pb^{a}/^{206}Pb^{a}$	2σ	Step age (Ga)	2σ	Grain age (Ga)	2σ
Jari Domain												
Jari-Guaribas Complex/enderbitic gneiss (sample JM-60)												
JM60/01	1450	12	5952	0.0950	1040	0.2219	0.2189	163	2973	12		
	1500	38	27,778	0.1105	64	0.2090	0.2087	41	2896	3		
	1550	40	38,462	0.0939	42	0.2168	0.2164	54	2955	4	2955	4
JM60/02	1450	32	6623	0.2200	128	0.1896	0.1875	47	2720	4		
	1500	32	45,455	0.1609	42	0.1932	0.1930	40	2769	3		
	1550	38	55,556	0.1770	46	0.1946	0.1943	29	2779	2	2779	2
JM60/03	**1500**	**36**	**19,608**	**0.0605**	**76**	**0.2582**	**0.2575**	**51**	**3232**	**3**		
	1550	**8**	**27,027**	**0.0984**	**55**	**0.2598**	**0.2594**	**174**	**3244**	**11**	**3233**	**6**
JM60/04	1450	34	111,111	0.0627	53	0.2459	0.2459	43	3159	3		
	1500	8	>1,000,000	0.1234	60	0.2491	0.2491	193	3180	12	3180	12
JM60/05	**1450**	**8**	**>1,000,000**	**0.0566**	**67**	**0.2470**	**0.2470**	**127**	**3166**	**8**		
	1500	**36**	**200,000**	**0.0886**	**70**	**0.2583**	**0.2583**	**63**	**3237**	**4**	**3237**	**4**
JM60/06	1450	36	200,000	0.1025	81	0.1948	0.1948	50	2783	4		
	1500	36	>1,000,000	0.1229	190	0.1945	0.1945	47	2780	4		
	1550	8	>1,000,000	0.1576	149	0.1953	0.1953	109	2787	9	2782	3
JM60/07	1450	38	66,667	0.0666	44	0.2532	0.2531	36	3204	2		
	1500	24	76,923	0.0544	17	0.2531	0.2530	57	3204	4		
	1550	**36**	**23,810**	**0.0636**	**66**	**0.2600**	**0.2596**	**48**	**3245**	**3**	**3245**	**3**
JM60/08	1550	36	200,000	0.1294	93	0.2261	0.2260	86	3025	6	3025	6
JM60/09	**1450**	**16**	**41,667**	**0.2239**	**520**	**0.1957**	**0.1954**	**64**	**2789**	**5**	**2789**	**5**
	1500	40	333,333	0.2147	61	0.1932	0.1932	33	2770	3		
JM60/10	**1450**	**8**	**41,667**	**0.3656**	**653**	**0.1956**	**0.1951**	**124**	**2786**	**10**		
	1500	**38**	**250,000**	**0.1928**	**74**	**0.1954**	**0.1954**	**60**	**2788**	**5**	**2788**	**5**
JM60/11	**1450**	**36**	**30,303**	**0.1467**	**59**	**0.1954**	**0.1951**	**49**	**2786**	**4**		
	1500	**40**	**111,111**	**0.1007**	**35**	**0.1953**	**0.1953**	**34**	**2787**	**3**		
	1550	**34**	**166,667**	**0.1190**	**79**	**0.1960**	**0.1960**	**37**	**2794**	**3**	**2789**	**5**
JM60/12	1450	36	125,000	0.1733	43	0.1868	0.1867	37	2714	3		
	1500	38	>1,000,000	0.1557	42	0.1891	0.1891	29	2735	2		
	1550	32	>1,000,000	0.1688	116	0.1920	0.1920	77	2760	7	2760	7
JM60/13	1450	36	22,727	0.2152	191	0.1935	0.1930	40	2769	3		
	1500	36	>1,000,000	0.2237	55	0.1926	0.1926	40	2765	3		
	1550	**40**	**125,000**	**0.2522**	**65**	**0.1954**	**0.1953**	**44**	**2787**	**4**	**2787**	**4**
JM60/14	1450	16	26,316	0.1394	200	0.1920	0.1914	42	2755	4		
	1500	**32**	**52,632**	**0.1009**	**96**	**0.1953**	**0.1952**	**42**	**2786**	**4**	**2786**	**4**
JM60/15	1500	36	66,667	0.1980	60	0.1915	0.1913	24	2753	2		
	1550	38	47,619	0.1972	80	0.1924	0.1921	46	2761	4	2761	4
Mean age (grains Z9+Z10+Z11+Z13+Z14—244 ratios—USD 1.5)									**2788±2 Ma**			
Mean age (grains Z3+Z5+Z7—116 ratios—USD 3.5)									**3238±6 Ma**			
Jari-Guaribas Complex/enderbitic gneiss (sample MV-27A)												
MV27A/4	1500	32	5917	0.0522	43	0.1811	0.17917	66	2646	6	2646	6
MV27A/5	1450	38	5747	0.0544	129	0.1831	0.18111	25	2663	2		
	1500	8	7246	0.1557	82	0.1930	0.19134	57	2754	5	2754	5
MV27A/6	1450	36	12,821	0.0378	26	0.1895	0.18847	25	2729	2	2729	2
MV27A/9	1450	8	8621	0.0254	48	0.1635	0.16206	128	2478	13	2478	13
MV27A/11	1450	16	5376	0.0724	134	0.1859	0.18377	79	2688	7	2688	7
MV27A/12	**1500**	4	**16,949**	**0.0366**	**59**	**0.1950**	**0.19428**	**220**	**2779**	**19**	**2779**	**19**
MV27A/14	**1450**	8	**11,905**	**0.0197**	**61**	**0.1960**	**0.1950**	**64**	**2785**	**5**	**2785**	**5**
MV27A/16	**1450**	36	**4739**	**0.0888**	**36**	**0.1987**	**0.19618**	**53**	**2795**	**4**	**2795**	**4**
Mean age (3 grains—48 ratios—USD 2.3)									**2790±8 Ma**			
Guianense Complex/monzogranitic gneiss (sample LT-126A)												
LT126A/1	1450	38	8547	0.1382	172	0.1781	0.17669	38	2622	4		
	1500	36	12,987	0.1306	188	0.1769	0.17594	66	2615	6	2621	6
LT126A/2	1450	30	2732	0.1444	82	0.1528	0.14809	56	2324	6		
	1500	26	76,923	0.1416	102	0.1754	0.17523	30	2609	3		
	1550	36	50,000	0.1526	50	0.1764	0.17611	33	2617	3	2617	3
LT126A/3	1450	38	4386	0.2095	460	0.1628	0.15981	228	2454	24		
	1500	38	23,810	0.1869	42	0.1763	0.17573	21	2613	2	2613	2
LT126A/4	1450	16	15,873	0.1480	62	0.1727	0.17189	82	2576	8		
	1500	**38**	**83,333**	**0.1402**	**43**	**0.1776**	**0.17749**	**23**	**2630**	**2**		

(continued on next page)

Table 1 (*continued*)

Zircon grain	T (°C)	No. of ratios	$^{206}Pb/^{204}Pb$	$^{208}Pb/^{206}Pb$	2σ	$^{207}Pb/^{206}Pb$	$^{207}Pb^{a}/^{206}Pb^{a}$	2σ	Step age (Ga)	2σ	Grain age (Ga)	2σ
	1550	**38**	**90,909**	**0.1429**	**34**	**0.1773**	**0.17728**	**39**	**2628**	**4**	**2629**	2
LT126A/5	1450	38	12,821	0.1282	88	0.1745	0.17353	37	2592	4		
	1500	**36**	**47,619**	**0.1347**	**39**	**0.1775**	**0.17723**	**40**	**2627**	**4**	**2627**	**4**
LT126A/6	1450	16	4651	0.0750	197	0.1662	0.16344	73	2492	8	2492	8
LT126A/7	1450	28	16,949	0.0756	153	0.1755	0.17471	62	2604	6		
	1500	**34**	**200,000**	**0.0630**	**20**	**0.1770**	**0.17693**	**38**	**2624**	**4**	**2624**	4
Mean age (3 grains—146 ratios—USD 1.5)									**2628**±2 Ma			
Noucouru Intrusive Suite/mesoperthite-granite (sample LT-218)												
LTR218/1	1485	36	31,250	0.1033	27	0.1790	0.17863	24	2641	2	2641	2
LTR218/4	1500	30	6897	0.1190	67	0.1799	0.1780	63	2635	6	2635	6
LTR218/5	1500	4	6211	0.1245	255	0.1811	0.17915	47	2645	4	2645	4
LTR218/6	1500	38	15,625	0.1081	32	0.1771	0.17626	28	2618	3	2618	3
	1530	34	17,544	0.1059	30	0.1758	0.1752	46	2608	4		
LTR218/7	1500	36	3367	0.1177	55	0.1812	0.17726	80	2628	7	2628	7
LTR218/9	**1500**	**36**	**2551**	**0.1242**	**64**	**0.1849**	**0.18011**	**38**	**2654**	**3**	**2654**	**3**
LTR218/11	1450	34	2865	0.1106	75	0.1804	0.17612	134	2617	13		
	1500	**30**	**13,889**	**0.1110**	**32**	**0.1815**	**0.18071**	**34**	**2660**	**3**	**2660**	**3**
LTR218/12	**1500**	**34**	**5525**	**0.1205**	**33**	**0.1822**	**0.1800**	**41**	**2653**	**4**	**2653**	**4**
Mean age (3 grains—100 ratios—USD 2.2)									**2656±4 Ma**			
Noucouru Inrusive Suite/mesoperthite-granite (sample NR-39)												
NR39/1	1500	28	14,085	0.1084	87	0.1783	0.17739	37	2629	3	2629	3
NR39/2	1450	36	15,385	0.0825	247	0.1684	0.16759	131	2534	13		
	1450	47	33,333	0.0858	56	0.1689	0.16847	18	2543	2		
	1500	40	35,714	0.1070	71	0.1772	0.17686	25	2624	2	2624	2
NR39/3	1500	38	27,778	0.0963	37	0.1778	0.17736	27	2629	3	2629	3
NR39/4	1450	38	7299	0.1047	61	0.1767	0.17471	36	2604	3		
	1500	36	31,250	0.1182	29	0.1791	0.17866	39	2641	4	2641	4
NR39/5	1450	10	10,870	0.0941	143	0.1768	0.17527	47	2609	4		
	1500	36	25,000	0.0985	33	0.1761	0.17556	23	2612	2	2611	2
NR39/6	1450	36	4484	0.0985	103	0.1669	0.16451	180	2503	18		
	1500	26	37,037	0.1137	43	0.1785	0.17817	23	2636	2	2636	2
NR39/7	1450	4	5714	0.0908	83	0.1744	0.17219	47	2579	5		
	1450	38	13,514	0.0920	62	0.1788	0.1780	50	2635	5		
	1500	**32**	**28,571**	**0.0941**	**47**	**0.1802**	**0.17982**	**43**	**2651**	**4**	**2651**	**4**
NR39/10	1450	14	6944	0.0946	263	0.1748	0.17284	62	2586	6		
	1485	**40**	**76,923**	**0.1005**	**103**	**0.1796**	**0.1794**	**93**	**2648**	**9**	**2648**	**9**
	1500	**40**	**21,277**	**0.1216**	**85**	**0.1800**	**0.17943**	**32**	**2648**	**3**	**2648**	**3**
Mean age (2 grains—112 ratios—USD 1.1)									**2649±2 Ma**			
Noucouru Intrusive Suite/charnockite (sample MV-18A)												
MV18A/1	1450	30	2841	0.1032	38	0.1699	0.1656	57	2514	6	2514	6
MV18A/3	1450	34	3165	0.0961	65	0.1709	0.16674	94	2525	9		
	1500	24	6329	0.1143	169	0.1792	0.17693	47	2625	4	2625	4
MV18A/6	1450	34	5525	0.0838	61	0.1587	0.15636	97	2417	11	2417	11
MV18A/7	1500	34	8772	0.1208	38	0.1708	0.16941	22	2552	2	2552	2
MV18A/8	1450	34	6250	0.0933	44	0.1655	0.16338	108	2491	11		
	1500	36	25,000	0.0891	38	0.1752	0.17464	23	2603	2	2603	2
MV18A/9	1450	16	3175	0.0942	51	0.1695	0.16557	137	2514	14		
	1500	32	5747	0.0861	108	0.1706	0.16844	31	2542	3	2542	3
MV18A/10	1450	6	3300	0.0972	162	0.1695	0.16572	58	2515	6	2515	6
MV18A/11	1450	6	33,333	0.0881	151	0.1611	0.16071	71	2463	7		
	1500	22	32,258	0.0934	42	0.1667	0.16644	30	2522	3	2522	3
Granitoids/monzogranite (sample LT-114)												
LT114/1	1500	38	2639	0.15759	77	0.14355	0.13853	26	2209	3	2209	3
LT114/2	**1500**	**20**	**2801**	**0.1531**	**183**	**0.1435**	**0.13906**	**33**	**2216**	**4**	**2216**	**4**
LT114/5	**1500**	**32**	**3311**	**0.1456**	**236**	**0.1432**	**0.13924**	**26**	**2218**	**3**	**2218**	**3**
LT144/09	1500	34	14,286	0.1783	156	0.1385	0.1376	60	2197	8	2197	8
LT114/10	1450	38	2740	0.0880	44	0.1432	0.13831	31	2206	4	2206	4
LT114/11	1500	22	2564	0.1788	85	0.1413	0.13576	170	2174	22	2174	22
LT114/12	**1500**	**8**	**5682**	**0.1574**	**203**	**0.1413**	**0.1390**	**166**	**2215**	**21**	**2215**	**21**
LT114/15	1500	38	4386	0.1081	29	0.1410	0.1379	25	2201	3	2201	3
LT114/17	**1500**	**6**	**6623**	**0.0947**	**148**	**0.1417**	**0.13977**	**65**	**2225**	**8**	**2225**	**8**
Mean age (4 grains—66 ratios—USD 1.1)									**2218±3 Ma**			

Table 1 (*continued*)

Zircon grain	T (°C)	No. of ratios	$^{206}Pb/^{204}Pb$	$^{208}Pb/^{206}Pb$	2σ	$^{207}Pb/^{206}Pb$	$^{207}Pb^{a}/^{206}Pb^{a}$	2σ	Step age (Ga)	2σ	Grain age (Ga)	2σ
Granitoids/monzogranite (sample EK-89)												
EK89/02	1450	8	5319	0.1452	348	0.1379	0.13544	131	2170	17	2170	17
EK89/03	1450	28	4292	0.0963	120	0.1539	0.15065	181	2354	20		
	1500	38	20,833	0.1105	39	0.1741	0.17351	21	2592	2	2592	2
	1550	32	15,625	0.1158	30	0.1720	0.17118	44	2570	4		
EK89/6	**1500**	**38**	**41,667**	**0.1548**	**69**	**0.1373**	**0.13692**	**31**	**2189**	**4**	**2189**	**4**
EK89/10	1450	16	3268	0.1705	1683	0.1355	0.13161	51	2120	7	2120	7
EK89/11	**1500**	**32**	**11,364**	**0.1612**	**166**	**0.1376**	**0.13654**	**22**	**2184**	**3**	**2184**	**3**
EK89/16	**1500**	**34**	**6711**	**0.2073**	**48**	**0.1384**	**0.13638**	**35**	**2182**	**4**	**2182**	**4**
Mean age (3 grains—104 ratios—USD 1.8)									**2185±4 Ma**			
Parintins Intrusive Suite/monzogranite (sample JM-25)												
JMR25/1	1450	36	4525	0.1255	94	0.1291	0.12572	71	2039	10		
	1500	**32**	**22,222**	**0.1805**	**699**	**0.1271**	**0.12656**	**33**	**2051**	**5**	**2051**	**5**
JMR25/2	1500	30	41,667	0.1404	111	0.1334	0.13316	61	2140	8	2140	8
JMR25/3	1450	30	2770	0.0912	161	0.1431	0.13844	50	2208	6	2208	6
JMR25/4	1450	16	3226	0.1488	255	0.1265	0.12238	60	1992	9		
	1500	**30**	52,632	**0.3638**	**206**	**0.1266**	**0.12633**	**26**	**2048**	**4**	**2048**	**4**
JMR25/6	1450	34	2513	0.2100	176	0.1296	0.12431	67	2019	10		
	1500	**36**	**10,101**	**0.3258**	**133**	**0.1274**	**0.12612**	**24**	**2045**	**3**	**2045**	**3**
JMR25/8	**1500**	**30**	**32,258**	**0.2502**	**108**	**0.1271**	**0.12668**	**31**	**2053**	**4**	**2053**	**4**
JMR25/9	**1485**	**22**	**9259**	**0.2245**	**69**	**0.1281**	**0.12666**	**31**	**2052**	**4**	**2052**	**4**
JMR25/12	1500	32	7092	0.1370	202	0.1277	0.1259	24	2042	3	2042	3
Mean age (5 grains—150 ratios—USD 1.8)									**2049±3 Ma**			
Granitoids/syenogranite (sample LT-17)												
LT17/4	**1500**	**38**	**2833**	**0.3520**	**99**	**0.1303**	**0.12532**	**38**	**2034**	**5**	**2034**	**5**
LT17/6	**1500**	**38**	**7299**	**0.2966**	**187**	**0.1269**	**0.12511**	**17**	**2031**	**2**	**2031**	**2**
LT17/7	**1500**	**40**	**4902**	**0.1717**	**96**	**0.1278**	**0.1251**	**26**	**2030**	**4**	**2030**	**4**
LT17/10	**1500**	**10**	**23,810**	**0.2915**	**124**	**0.1261**	**0.12576**	**72**	**2040**	**10**	**2040**	**10**
LT17/13	**1500**	**30**	**5236**	**0.3251**	**91**	**0.1273**	**0.12485**	**32**	**2027**	**5**	**2027**	**5**
LT17/14	**1500**	**22**	**6452**	**0.3406**	**102**	**0.1269**	**0.12481**	**34**	**2026**	**5**		
	1550	**28**	**6289**	**0.3711**	**97**	**0.1270**	**0.1250**	**48**	**2028**	**7**	**2027**	**4**
Mean age (6 grains—206 ratios—USD 1.3)									**2030±2 Ma**			
Carecuru Domain												
Paru-Maratiá Complex/granodioritc gneiss (sample MV-65A)												
MV65A/1	1450	40	2513	0.0932	100	0.1241	0.11877	46	1938	7		
	1480	40	12,821	0.1148	37	0.1369	0.1360	27	2177	3	2177	3
MV65A/2	1450	40	10,526	0.0282	28	0.1308	0.12942	54	2090	7		
	1500	**30**	33,333	**0.1123**	**37**	**0.1375**	**0.13707**	**22**	**2191**	**3**	**2191**	**3**
MV65A/4	1450	30	4082	0.0687	140	0.1336	0.13035	48	2103	7		
	1500	**34**	52,632	**0.0893**	**25**	**0.1373**	**0.1370**	**39**	**2190**	**5**	**2190**	**5**
MV65A/5	1450	8	9259	0.0795	52	0.1962	0.19493	75	2784	6	2784	6
	1500	8	>1,000,000	0.1044	57	0.1900	0.1900	88	2742	8		
MV65A/6	1450	6	5814	0.0864	140	0.1376	0.13538	59	2169	8	2169	8
MV65A/7	1450	32	10,000	0.0552	102	0.1319	0.13065	18	2107	2	2107	2
MV65A/9	1450	8	4016	0.0691	210	0.1328	0.12948	90	2091	12	2091	12
MV65A/10	1450	40	16,949	0.0716	210	0.1330	0.13224	20	2128	3		
	1500	**34**	43,478	**0.1133**	**57**	**0.1374**	**0.13709**	**57**	**2191**	**7**	**2191**	**7**
MV65A/13	1550	36	4386	0.0377	151	0.1303	0.12739	34	2063	5	2063	5
Mean age (3 grains—98 ratios—USD 0.2)									**2191±2 Ma**			
Carecuru Intrusive Suite/diorite (sample LT-193)												
LT193/1	1500	8	41,667	0.1574	631	0.1307	0.13036	446	2103	60		
	1500	**20**	37,037	**0.1663**	**132**	**0.1333**	**0.1330**	**39**	**2139**	**5**	**2139**	**5**
LT193/2	1450	28	5618	0.1635	96	0.1346	0.13216	33	2127	4		
	1500	**36**	12195	**0.1760**	**143**	**0.1338**	**0.13276**	**45**	**2135**	**6**	**2135**	**6**
LT193/3	**1450**	**24**	9901	**0.1526**	**286**	**0.1336**	**0.13279**	**24**	**2135**	**3**	**2135**	**3**
LT193/5	**1500**	**40**	14,085	**0.1654**	**84**	**0.1340**	**0.13297**	**19**	**2138**	**2**	**2138**	**2**
LT193/6	**1500**	**36**	50,000	**0.1666**	**111**	**0.1334**	**0.13315**	**35**	**2140**	**5**		
	1550	**34**	43,478	**0.1826**	**55**	**0.1339**	**0.13355**	**32**	**2145**	**4**	**2143**	5
LT193/7	**1450**	**36**	15,625	**0.1461**	**65**	**0.1338**	**0.13299**	**34**	**2138**	**4**		
	1500	**30**	35,714	**0.1804**	**125**	**0.1335**	**0.13309**	**46**	**2139**	**6**	**2139**	4

(continued on next page)

Table 1 (*continued*)

Zircon grain	T (°C)	No. of ratios	$^{206}Pb/^{204}Pb$	$^{208}Pb/^{206}Pb$	2σ	$^{207}Pb/^{206}Pb$	$^{207}Pb^{a}/^{206}Pb^{a}$	2σ	Step age (Ga)	2σ	Grain age (Ga)	2σ
Carecuru Intrusive Suite/diorite (sample LT-193)												
LT193/8	**1450**	**20**	**5917**	**0.1822**	**73**	**0.1347**	**0.13279**	**109**	**2135**	**14**		
	1500	**16**	8696	**0.1755**	**75**	**0.1353**	**0.13383**	**85**	**2149**	**11**	**2144**	**13**
Mean age (7 grains—292 ratios—USD 1.5)									**2139 ± 2 Ma**			
Granitoids/monzogranite (sample LT-177)												
LT177/1	**1550**	**10**	**10,753**	**0.1187**	**89**	**0.1376**	**0.13605**	**137**	**2178**	**18**	**2178**	**18**
LT177/3	**1500**	**32**	**26,316**	**0.1275**	**32**	**0.1366**	**0.13614**	**20**	**2179**	**3**	**2179**	**3**
LT177/5	1500	6	> 1,000,000	0.1292	62	0.1345	0.13445	134	2157	17	2157	17
LT177/6	**1450**	**18**	**3546**	**0.1489**	**90**	**0.1396**	**0.1360**	**71**	**2177**	**9**	**2177**	**9**
LT177/11	**1500**	**38**	**35,714**	**0.1285**	**176**	**0.1357**	**0.13533**	**52**	**2169**	**7**	**2169**	**7**
LT177/16	**1500**	**40**	**7407**	**0.1134**	**50**	**0.1377**	**0.13592**	**28**	**2176**	**4**	**2176**	**4**
Mean age (5 grains—138 ratios—USD 1.5)									**2177 ± 3 Ma**			
Granitoids/syenogranite (sample LT-207B)												
LT207B/2	1500	24	6452	0.0885	54	0.1314	0.1294	32	2090	4	2090	4
LT207B/4	1500	32	2688	0.0849	71	0.1336	0.1287	36	2081	5	2081	5
LT207B/5	**1500**	**32**	**5376**	**0.0850**	**63**	**0.1324**	**0.1300**	**21**	**2098**	**3**	**2098**	**3**
LT207B/15	**1500**	**32**	**7042**	**0.0919**	**44**	**0.1320**	**0.1300**	**18**	**2099**	**2**	**2099**	**2**
Mean age (2 grains—64 ratios—USD 0.5)									**2098 ± 2 Ma**			
Paru Domain												
Trondhjemitic gneiss (sample LT-191A)												
LT191A/1	1450	34	3401	0.1022	54	0.1350	0.13148	29	2118	4		
	1500	**38**	**24,390**	**0.1134**	**27**	**0.1344**	**0.13386**	**16**	**2150**	**2**		
	1550	**8**	**18,868**	**0.1134**	**139**	**0.1345**	**0.13381**	**95**	**2149**	**12**	**2149**	**2**
LT191A/2	1450	18	4926	0.1350	55	0.1353	0.13259	25	2133	3		
	1500	**34**	**26,316**	**0.0715**	**30**	**0.1345**	**0.13404**	**19**	**2152**	**2**	**2152**	**2**
LT191A/3	1450	32	10,204	0.0547	167	0.1316	0.13027	46	2102	6	2102	6
LT191A/4	1450	32	8333	0.0966	48	0.1337	0.13219	21	2128	3	2128	3
LT191A/5	**1500**	**34**	**31,250**	**0.0451**	**19**	**0.1335**	**0.13312**	**19**	**2140**	**2**		
	1550	**34**	**45,455**	**0.0505**	**50**	**0.1336**	**0.13331**	**21**	**2142**	**3**	**2141**	**2**
LT191A/9	1450	36	5128	0.0851	56	0.1291	0.12632	55	2048	8	2048	8
LT191A/14	**1500**	**28**	**6711**	**0.0565**	**57**	**0.1351**	**0.13323**	**26**	**2141**	**3**	**2141**	**3**
LT191A/15	1450	34	8621	0.1025	56	0.1330	0.13145	17	2118	2		
	1500	40	41,667	0.0880	45	0.1325	0.13213	23	2127	3	2127	3
LT191A/16	1450	34	43,478	0.0991	12	0.1324	0.13218	37	2127	5		
	1500	**8**	**111,111**	**0.0812**	**196**	**0.1332**	**0.13311**	**134**	**2140**	**18**	**2140**	**18**
Mean age (Z1 + Z2—80 ratios—USD 1.0)									**2150 ± 2 Ma**			
Mean age (Z5 + Z14 + Z16—104 ratios—USD 0.8)									**2141 ± 2 Ma**			
Igarapé Urucu Intrusive Suite/charnockite (sample LT-185A)												
LT185A/1	**1500**	**32**	**4405**	**0.1926**	**182**	**0.1314**	**0.12839**	**40**	**2076**	**5**	**2076**	**5**
LT185A/4	**1500**	**36**	**4329**	**0.2074**	**152**	**0.1305**	**0.12762**	**68**	**2066**	**9**	**2066**	**9**
LT185A/7	**1500**	**32**	**2564**	**0.2093**	**189**	**0.1343**	**0.12819**	**38**	**2074**	**5**	**2074**	**5**
LT185A/9	1500	36	2994	0.0994	25	0.1312	0.12661	26	2052	4	2052	4
Mean age (3 grains—92 ratios—USD 1.4)									**2074 ± 5 Ma**			

Values in bold were included in the age calculations.

[a] Radiogenic.

classically observed in magmatic zircons. The isotopic data were collected on 15 zircons, which yielded ages ranging from 2760 to 3245 Ma. Due to the wide spread of the data (485 Ma), two ages were calculated separately. Three zircon crystals with the oldest ages furnished a poorly constrained (USD = 3.5) mean value of 3238 ± 6 Ma, whereas an age of 2788 ± 2 Ma (USD = 1.5) was calculated with the other five grains. No relationships between shape and age of the grains have been observed.

These data permit two distinct interpretations: the age of 3.24 Ga represents the age of the igneous protolith and the age of 2.79 Ga indicates the time of the high-grade metamorphic event. Alternatively, both ages can be assumed as igneous ages, but the oldest being provided by inherited grains. The second hypothesis should be more acceptable since, in both zircon populations some crystals gave the same age at different steps of heating (e.g. grains JM60/03, JM60/06, JM60/10 and JM60/11), indicating that the zircon crystals registered individually a single geological event. In addition, strong variations of the $^{208}Pb/^{206}Pb$ ratios compared to the $^{207}Pb/^{206}Pb$ ratios of these grains are observed, which may be interpreted to reflect Th/U zonation during magmatic growth (Klötzli, 1999). Then, the age of 2788 ± 2 Ma is interpreted as the age of the igneous precursor of the granulite and the age of 3238 ± 6 Ma is considered as inherited from an oldest magmatic event. Furthermore, new

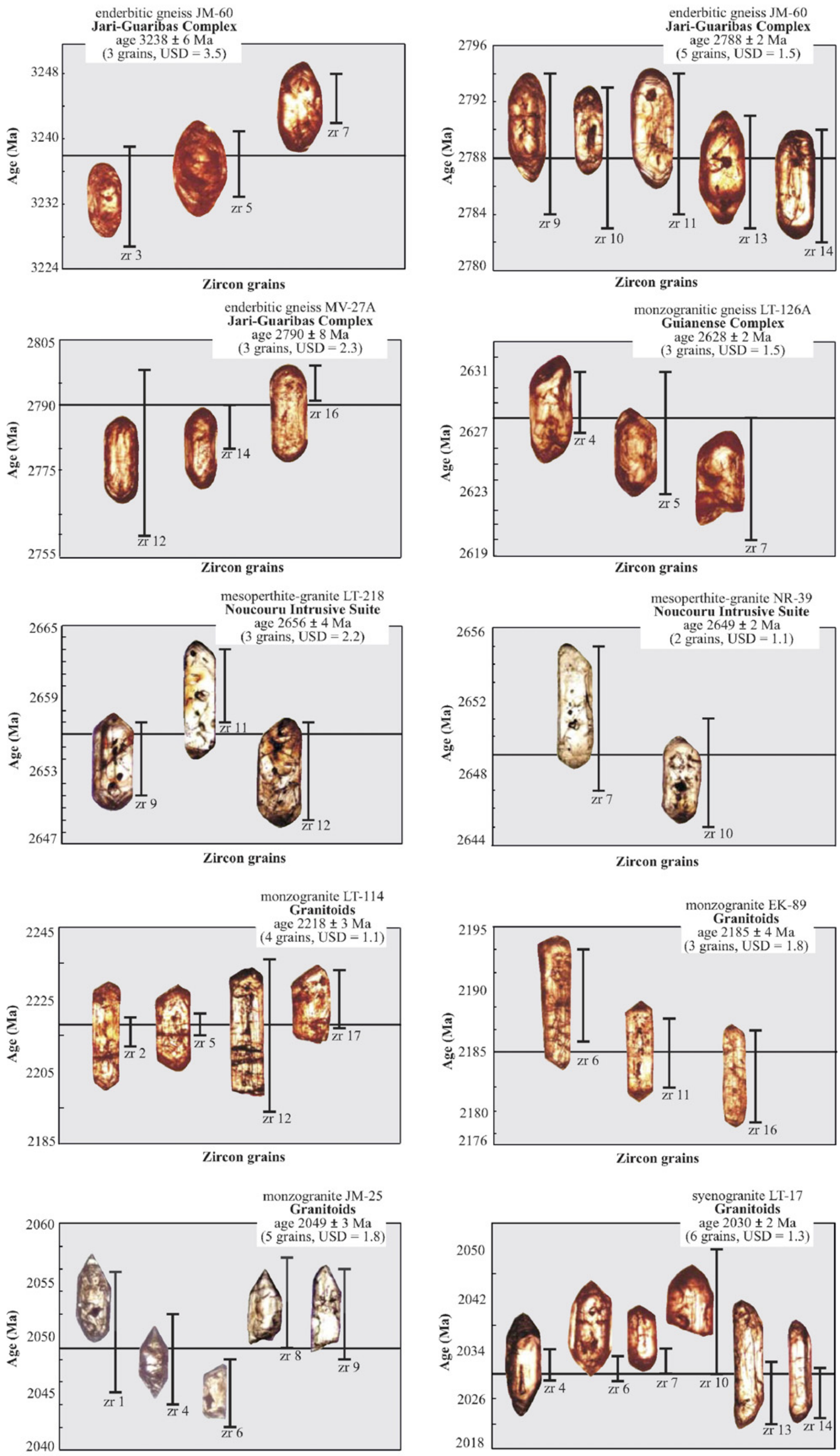

Fig. 3. Pb-evaporation diagrams for the dated samples from the Jari Domain. The error bars correspond to the mean age value for each zircon grain.

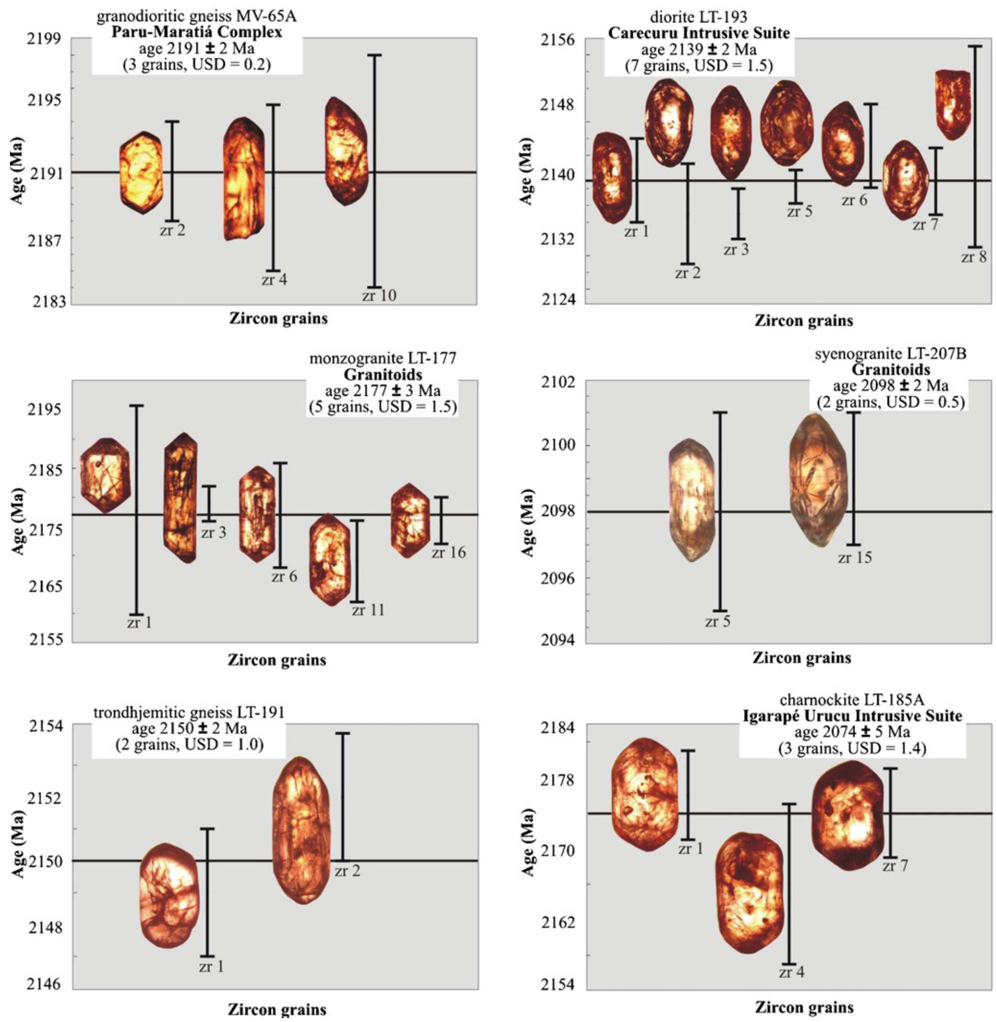

Fig. 4. Pb-evaporation diagrams for the dated samples from the Carecuru and Paru domains. The error bars correspond to the mean age value for each zircon grain.

geochronological data furnished by metamorphic zircon and monazite from granulites of the Jari-Guaribas Complex, dated the high-grade metamorphic event at about 2.1 Ga (Rosa-Costa et al., submitted for publication), reinforcing our interpretation.

The zircons from the enderbitic gneiss (MV-27A) are sub-euhedral, with external parts showing magmatic zoning. The eight grains provided ages between 2646±6 Ma and 2795±4 Ma at the higher steps of temperature. A mean age of 2790±8 Ma (USD=2.3) was calculated from three grains, which is similar to the previous sample, even if it is not as well defined as that, and it is alike interpreted as the crystallization age of the protolith of the granulite. The younger and variable ages given by the other five grains are assumed to represent perturbations of the U–Pb system in these zircons, induced by younger, probably Transamazonian related geological events.

These new geochronological data obtained for rocks from the Jari-Guaribas Complex reinforce the existence of two distinct magmatic events in the Jari Domain, occurred during the Paleoarchean (≈ 3.24 Ga) and at the Meso-Neoarchean transition (≈ 2.79–2.80 Ga), which have already been identified at 3321±11 Ma and 2797±3 Ma by Klein et al. (2003) and Rosa-Costa et al. (2003), respectively.

A monzogranitic gneiss (sample LT-126A) of the Guianense Complex was analyzed and the dated zircons are euhedral to sub-euhedral, with visible magmatic zoning in their external parts. Seven zircon crystals yielded ages between 2613±2 Ma and 2629±2 Ma at temperature steps of 1500 °C and 1550 °C. The three oldest crystals provided a mean value of 2628±2 Ma (USD=1.5), which is interpreted as giving the igneous age of the protolith. This age, added to the age of 2652±4 Ma previously obtained on a tonalitic gneiss from the same metamorphic complex (Rosa-Costa et al., 2003), confirms the existence of a Neoarchean magmatic event, at about 2.63–2.65 Ga, which is at about 150 Ma younger than the one identified in rocks from the Jari-Guaribas Complex.

Three different plutons of the Noucouru Intrusive Suite were investigated, with the goal of dating the catazonal magmatic event that characterizes this suite. The dated samples consist of mesoperthite-granites (samples LT-218 and NR-39) and of a true charnockite (sample MV-18A). Zircons from the three distinct samples show similar textural characteristics. They are sub-euhedral crystals, exhibiting magmatic zoning and containing several mineral inclusions (rounded and acicular) in their inner parts.

In the sample LT-218, eight zircon grains furnished ages ranging between 2618±3 Ma and 2660±3 Ma. Three crystals yielded a mean age of 2656±4 Ma (USD=2.2). This age, even poorly constrained, can be considered as a good indication of the time of the catazonal magmatic event, occurred at about 2.66 Ma. Concerning to the sample NR-39, eight grains gave ages varying between 2611±2 Ma and 2651±4 Ma, and the two oldest grains furnished a mean age of 2649±2 Ma, considered as a minimum age. In the sample MV-18A, eight grains yielded ages ranging from 2522±3 Ma to 2625±4 Ma at the highest steps of heating. As no reproducible ages were obtained, a mean age could not be calculated, and the oldest age of 2625±4 Ma is assumed as the minimum age for the crystallization of the rock.

This new set of ages, obtained from rocks of the Noucouru Intrusive Suite, is significantly older than the age of 2605±6 Ma furnished by a garnet-bearing enderbite of that suite, which was collected from a pluton located in the southern part of the Jari Domain (Ricci et al., 2002). The geochronological data suggest a protracted period, of about 50 Ma, for the catazonal magmatism or, alternatively, this magmatism has occurred in distinct pulses during Neoarchean times.

In order to provide geochronological constraints for the widespread granitic magmatism registered in the Jari Domain, zircon populations from four distinct plutons were analyzed (samples LT-114, EK-89, JM-25 and LT-17). The studied plutons show distinct mineralogical composition, mode of occurrence and intensity of deformation (see Appendix A).

Samples LT-114 and EK-89 were collected from two monzogranitic plutons located close to the boundary zone between the Jari and Carecuru Domains. The former comes from a pluton that was strongly affected by the deformation imparted by the Ipitinga Lineament and that intruded the metavolcano-sedimentary rocks of the Paleoproterozoic Ipitinga Group. The latter is intrusive into the Neoarchean gneisses of the Guianense Complex as well as into metavolcano-sedimentary rocks correlated to the Ipitinga Group.

In both samples, the zircon grains are euhedral, with well-developed pyramidal faces, and most of them are metamictic, showing transversal cracks and mineral inclusions. Several grains furnished high level of common lead ($^{206}Pb/^{204}Pb<2500$). Seventeen grains were analyzed from sample LT-114, and nine crystals yielded ages between 2174±22 Ma and 2225±8 Ma. A mean age of 2218±3 Ma (USD=1.1) was calculated with the four oldest grains, and considered as being the age of crystallization of the granite.

For the sample EK-89, 16 grains were analyzed and only 6 crystals provided useful isotopic results. Among these, five crystals gave ages between 2120±7 Ma and 2189±4 Ma. A mean age of 2185±4 Ma (USD=1.8) was calculated based on the three oldest grains, interpreted as the crystallization age. One grain yielded an age of 2592±2 Ma, attributed to inheritance from Archean source rocks.

The ages of 2218±3 Ma and 2185±4 Ma indicated the existence of eo-Transamazonian granitic magmatism events, not yet identified in other segments of the eastern Guiana Shield. For instance, in French Guiana, the period between 2.22 and 2.13 Ga is marked by tholeitic and calc-alkaline magmatic events, related, respectively, to stages of oceanization and magmatic arc building (Delor et al., 2003a).

The sample JM-25 came from a small monzogranitic pluton of the Parintins Intrusive Suite. The zircon grains are euhedral, with pyramidal faces, showing magmatic zoning and several mineral inclusions. A narrow range of values was provided by 6 crystals, with ages between 2042±3 Ma and 2053±4 Ma. A mean age of 2049±3 Ma (USD=1.8) was calculated with five crystals, interpreted as the time of crystallization of the granite. However, two grains gave older ages of 2140±8 Ma and 2208±6 Ma, and were considered as inherited crystals from reworked eo-Transamazonian source rocks.

The sample LT-17 was collected from a strongly mylonitized two-mica granite, emplaced along a NW–SE strike-slip zone that affects rocks of the Ipitinga Group and Guianense Complex. The zircon grains are clear, euhedral to sub-euhedral and some of them show few fractures and mineral inclusions in the inner parts. For this sample, six zircon grains furnished isotopic results only at the highest temperature steps. The ages vary from 2027±5 to 2040±10 Ma, producing a mean value of 2030±2 Ma (USD=1.3), interpreted as the age of the granite.

The ages of 2049±3 Ma and 2030±2 Ma furnished by the samples JM-25 and LT-17 date the youngest magmatic events in the Jari Domain and are related to late stages of evolution of the Transamazonian orogenic cycle.

3.2.1.2. Carecuru Domain. Zircon populations from four samples of gneisses and granitoids of the Carecuru Domain have been dated and only Paleoproterozoic ages were obtained, confirming the previous assumption of Rosa-Costa et al. (2003), which admitted a dominant Paleoproterozoic age pattern for this domain.

Two samples, one from the Paru-Maratiá Complex (MV-65A) and the other from the Carecuru Intrusive Suite (LT-193), were dated in order to better constrain the age of the calc-alkaline magmatism in the Carecuru Domain. The zircons from the granodioritic gneiss MV-65A are euhedral with pyramidal faces or sub-euhedral with rounded terminations, and some of them exhibit magmatic zoning. Nine zircon grains furnished isotopic results, and eight crystals yielded Paleoproterozoic ages between 2191±6 and 2063±5 Ma. The youngest ages were not considered for the age calculation. The three oldest grains provided a mean value of 2191±2 Ma (USD=0.2), interpreted as the crystallization age of the igneous protolith. One grain gave an age of 2784±6 Ma, interpreted as inheritance, indicating contamination of the Palaeoproterozoic magma with Archean rocks.

The zircon grains from the diorite LT-193 are clear, sub-euhedral, containing rare mineral inclusions and fractures. They exhibit contrasted fine zoning, as frequently observed in magmatic zircons. Seven among eight analyzed zircon grains yielded isotopic results, showing similar ages between the grains and, in some grains, between the heating steps. A mean age at 2139±2 Ma (USD=1.5) was calculated, considered as the crystallization age, which is in good agreement with the age of

2140 ± 1 Ma, previously obtained on a diorite of the same suite (Rosa-Costa et al., 2003). No Archean component has been found in this sample.

These new data extend the time span for the calc-alkaline magmatism in the Carecuru Domain. Previous results furnished ages of 2.15 Ga and 2.14 Ga for this magmatism (Rosa-Costa et al., 2003). According to the geochronological results, the time between 2.19 and 2.14 Ga could represent a protracted period of calc-alkaline magmatism or, alternatively, two distinct pulses, occurring at about 2.19 Ga and at 2.15–2.14 Ga, the latter being the preferred interpretation. Anyway, the results are in good agreement with the two phases of calc-alkaline magmatism at 2.18–2.16 Ga and at 2.15–2.13 Ga, related to a magmatic arc context, characterized in French Guiana (Delor et al., 2003a).

As in the Jari Domain, several plutons of granitoids were characterized in the Carecuru Domain, which are constituted mainly of monzogranites and syenogranites, and display distinct structural characteristics, varying from weakly deformed to mylonitic.

Two granitic plutons (samples LT-177 and LT-207B) were dated, in order to compare the granitic magmatism chronology between the different domains during the Transamazonian orogenic cycle. The sample LT-177 corresponds to a weakly deformed monzogranite, while sample LT-207B consists of a mylonitic syenogranite. Zircon grains from the sample LT-177 are euhedral, with well-developed pyramidal faces, exhibiting magmatic zoning and transversal fractures, being frequently broken. Zircon crystals from the granite LT-207B are sub-euhedral, often fractured and metamictic, although some of them are clear, with visible magmatic zoning. In both samples, 16 crystals were selected for analysis, but, due to the metamictic nature of most of them, only six and four grains, respectively, furnished $^{206}Pb/^{204}Pb$ ratio > 2500.

Two diachronous granitic pulses were revealed by the dated samples. The zircon crystals of the monzogranite LT-177 provided values between 2157 ± 17 Ma and 2179 ± 3 Ma. A mean age of 2177 ± 3 Ma (USD = 1.5) was calculated with the five oldest grains, and interpreted as the crystallization age. This monzogranite is slightly younger than the calc-alkaline magmatic pulse dated at about 2.19 Ga, suggesting that it can represent more evolved rocks from the calc-alkaline series.

The four grains from the sample LT-207B yielded ages ranging from 2081 ± 5 to 2099 ± 2 Ma. A mean age of 2098 ± 2 Ma was calculated with only two zircons, which is considered as the minimum age of crystallization. In French Guiana, this period also corresponds to a phase of granitic magmatism, with emplacement of plutons along shear zones, during a stage of oblique plate convergence.

3.2.1.3. Paru Domain. In this domain, two samples were investigated. The first one is a trondhjemitic gneiss (sample LT-191A) enclosed within the granulites from the Ananaí Complex, and the second one is a charnockite (sample LT-185A) from the Igarapé Urucu Intrusive Suite.

Zircon crystals from the trondhjemitic gneiss LT-191A are sub-euhedral with rounded terminations and fractured. In some grains magmatic zoning is visible. Eight grains furnished isotopic results and seven of them yielded ages between 2127 ± 3 Ma and 2152 ± 2 Ma in high steps of temperature. Three crystals yielded a mean value of 2141 ± 2 Ma, while a mean age of 2150 ± 2 Ma could be calculated with two other crystals. The latter is interpreted as the minimum age of crystallization of the igneous precursor. Such an age is similar to the age of 2.15–2.14 Ga of the calc-alkaline magmatism, characterized in the Carecuru Domain (Rosa-Costa et al., 2003 and this work).

The zircon grains from the charnockite LT-185A are typically rounded grains, showing magmatic zoning in the inner parts, with few mineral inclusions and often strongly metamictic. Among analyzed 12 grains, only four furnished useful isotopic results. The ages range from 2052 ± 4 Ma to 2076 ± 5 Ma and the three oldest grains provided a mean age of 2074 ± 5 Ma (USD = 1.4), interpreted as the crystallization age. Although defined on a small number of grains, this age constrains the timing of the Paleoproterozoic charnockitic magmatism of the Igarapé Urucu Intrusive Suite, better than the previous geochronological dating available for this unit that furnished strongly variable ages, between 2161 ± 3 Ma and 2064 ± 4 Ma (Rosa-Costa et al., 2003). The new age at 2074 ± 5 Ma is in agreement with the late-Transamazonian charnockitic magmatic events, dated between 2.07 and 2.05 Ga in other segments of the eastern Guiana Shield and considered as indicators of the time of the high-grade metamorphism (Avelar et al., 2001; Lafon et al., 2001; Roever et al., 2003).

3.2.2. Sm–Nd isotopic data — identifying events of crustal growth or reworking

The Sm–Nd isotopic results furnished by 32 samples are given in Table 2. As all samples showed $^{147}Sm/^{144}Nd$ ratios in the range of 0.08 to 0.13, the data were useful for calculation of T_{DM} model ages. In order to verify the reproducibility of the Sm–Nd isotopic analyses, the sample LT-207B was analyzed in duplicate and no differences of the Sm–Nd concentrations and isotopic composition were observed between the two analyses. The Table 2 also includes initial ε_{Nd} values, calculated with the age of the emplacement provided by zircon Pb-evaporation method, obtained in this work or compiled from literature. When the zircon ages are not available, an estimation of the age is assumed, based on stratigraphic correlations.

3.2.2.1. Jari Domain. Sixteen samples were investigated, representing two major groups of rock: the Archean metamorphic complexes and the Paleoproterozoic granitoids. The T_{DM} model ages are clearly different between the two groups, as displayed in the ε_{Nd} vs. time diagram (Fig. 5A).

The first group includes samples from Archean metamorphic complexes (Jari-Guaribas, Baixo Mapari and Guianense) and igneous charnockites of the Noucouru Intrusive Suite, which provided T_{DM} model ages ranging from 3.26 to 2.83 Ga, predominating ages between 3.26 and 2.92 Ga, and negative ε_{Nd} values, between − 3.97 and − 0.17. This range of model ages is in accordance with previous Nd data acquired in other Archean segments of the Guiana Shield, in its southeastern sector (3.06–3.01 Ga—Sato and Tassinari, 1997; 3.36–3.07 Ga—Pimentel et al., 2002; 3.29–2.90 Ga—Avelar et al., 2003) and northern sector (Imataca Complex: 3.23–2.80 Ga—Tassinari et al., 2001, 2004).

Table 2
Whole rock Sm–Nd isotopic data from the studied samples

Lithology/sample	Stratigrafic unit	Sm (ppm)	Nd (ppm)	$^{147}Sm/^{144}Nd$	$^{143}Nd/^{144}Nd$	2σ (10^{-5})	f (Sm/Nd)	$\varepsilon_{Nd}(0)$	Zircon age (Ga)	Ref.	T_{DM} (Ga)	$\varepsilon_{Nd}(t)$
Jari Domain												
Enderbitic gneiss/JM-60		5.21	34.91	0.09022	0.510475	2	−0.5413	−42.19	2.79	1	3.21	−3.97
Enderbitic gneiss/MV-48	Jari-Guaribas Complex	7.40	37.88	0.11810	0.511032	1	−0.3996	−31.33	2.80	2	3.26	−3.12
Enderbitic gneiss/MV-27A		4.17	23.78	0.10601	0.510820	4	−0.4611	−35.46	2.79	1	3.19	−2.91
Granitic gneiss/MV-39B	Baixo Mapari Complex	18.94	104.68	0.10941	0.510940	0.4	−0.4438	−33.12	2.65	3	3.12	−3.38
Mesoperthite-granite/LT-218		17.17	86.33	0.12025	0.511207	1	−0.3887	−27.91	2.65	1	3.04	−1.86
Mesoperthite-granite/LT-213		17.83	93.61	0.11515	0.511103	2	−0.4146	−29.94	2.65	3	3.04	−2.15
Charnoenderbite/JM-07	Noucouru Intrusive Suite	11.5	60.88	0.11424	0.511115	1	−0.4192	−29.71	2.60	4	2.99	−2.14
Charnockite/MV-18A		12.97	70.28	0.11156	0.511049	1	−0.4328	−31.00	2.62	1	3.01	−2.31
Granodiotitic gneiss/LT-40		5.28	35.59	0.08976	0.510760	1	−0.5437	−36.63	2.65	2	2.83	−0.17
Monzogranitic gneiss/LT-126A	Guianense Complex	6.45	40.94	0.09520	0.510784	1	−0.5160	−36.17	2.63	1	2.94	−1.87
Tonalitic gneiss/LT-123A		2.33	14.80	0.09538	0.510796	2	−0.5151	−35.93	2.63	3	2.92	−1.65
Granodioritic gneiss/LT-11A		14.95	85.93	0.10519	0.510939	0.6	−0.4652	−33.14	2.65	3	2.99	−1.95
Monzogranite/EK-89		5.40	36.62	0.08917	0.511169	0.8	−0.5467	−28.66	2.18	1	2.30	1.47
Alkali feldspar-granite/MV-07	Granitoids	16.97	90.70	0.11308	0.511415	0.8	−0.4251	−23.86	2.15	1	2.48	−0.87
Syenogranite/LT-17		4.48	23.55	0.11510	0.511424	1	−0.4148	−23.68	2.03	1	2.52	−2.42
Monzogranite/JM-25	Parintins Intrusive Suite	4.89	34.43	0.08591	0.511000	1	−0.5632	−31.95	2.05	1	2.45	−2.51
Carecuru Domain												
Granodioritic gneiss/MV-65A		2.87	14.46	0.12003	0.511543	0.8	−0.3898	−21.36	2.19	3	2.45	0.22
Granodioritic gneiss/LT-206A		1.77	14.27	0.07507	0.510886	3	−0.6184	−34.18	2.15	3	2.38	−0.58
Tonalitic gneiss/LT-202A	Paru-Maratiá Complex	4.45	22.87	0.11773	0.511512	7	−0.4015	−21.96	2.15	2	2.44	−0.15
Dioritic gneiss/LT-196B		4.36	23.67	0.11135	0.511422	3	−0.4339	−23.72	2.15	3	2.43	−0.15
Diorite/LT-193	Carecuru Intrusive Suite	3.37	17.56	0.11595	0.511583	2	−0.4105	−20.58	2.14	1	2.28	1.63
Diorite/LT-76		3.89	19.61	0.11983	0.511512	0.5	−0.3908	−21.96	2.14	2	2.50	−0.84
Metavolcanic/LT-182C	Supracrustal Sequences	7.80	45.67	0.10326	0.511311	0.8	−0.4750	−25.89	2.14	3	2.40	−0.20
Metavolcanic/LT-61A		6.18	28.99	0.12890	0.511664	2	−0.3447	−19.00	2.14	3	2.49	−0.36
Monzogranite/LT-177		6.65	40.65	0.09895	0.511199	1	−0.4969	−28.07	2.17	1	2.46	−0.69
Syenogranite/LT207B	Granitoids	2.85	16.87	0.10211	0.510993	1	−0.4809	−32.09	2.1	1	2.83	−6.61
Syenogranite/LT-207B		2.91	17.11	0.10274	0.51101	4	−0.4777	−31.76	2.1	1	2.82	−6.45
Monzogranite/LT-201		3.54	19.88	0.10776	0.511382	0.8	−0.4522	−24.50	2.1	3	2.40	−0.51
Paru Domain												
Enderbitic gneiss/MV-70D	Ananaí Complex	3.24	24.64	0.07963	0.510571	1.5	−0.5952	−40.32	2.6	2	2.83	−1.16
Trondhjemitic gneiss/LT-191A		0.90	5.10	0.10612	0.511415	2	−0.4605	−23.86	2.15	1	2.32	1.17
Charnockite/LT-185A	Igarapé Urucu Intrusive Suite	24.62	165.49	0.08993	0.510938	2	−0.5428	−33.16	2.07	1	2.61	−4.80
Charnockite/MV-71A		7.29	48.24	0.09138	0.510909	0.5	−0.5354	−33.73	2.06	2	2.68	−5.89
Charnockite/MV-68A		27.61	198.88	0.08394	0.51082	2	−0.5733	−35.46	2.07	1	2.63	−5.51

T_{DM} ages were calculated using the DePaolo (1981) model for Nd evolution of the depleted mantle.
References for the crystallization ages: (1) this work, (2) Rosa-Costa et al. (2003), (3) estimated age, (4) Ricci et al. (2002).

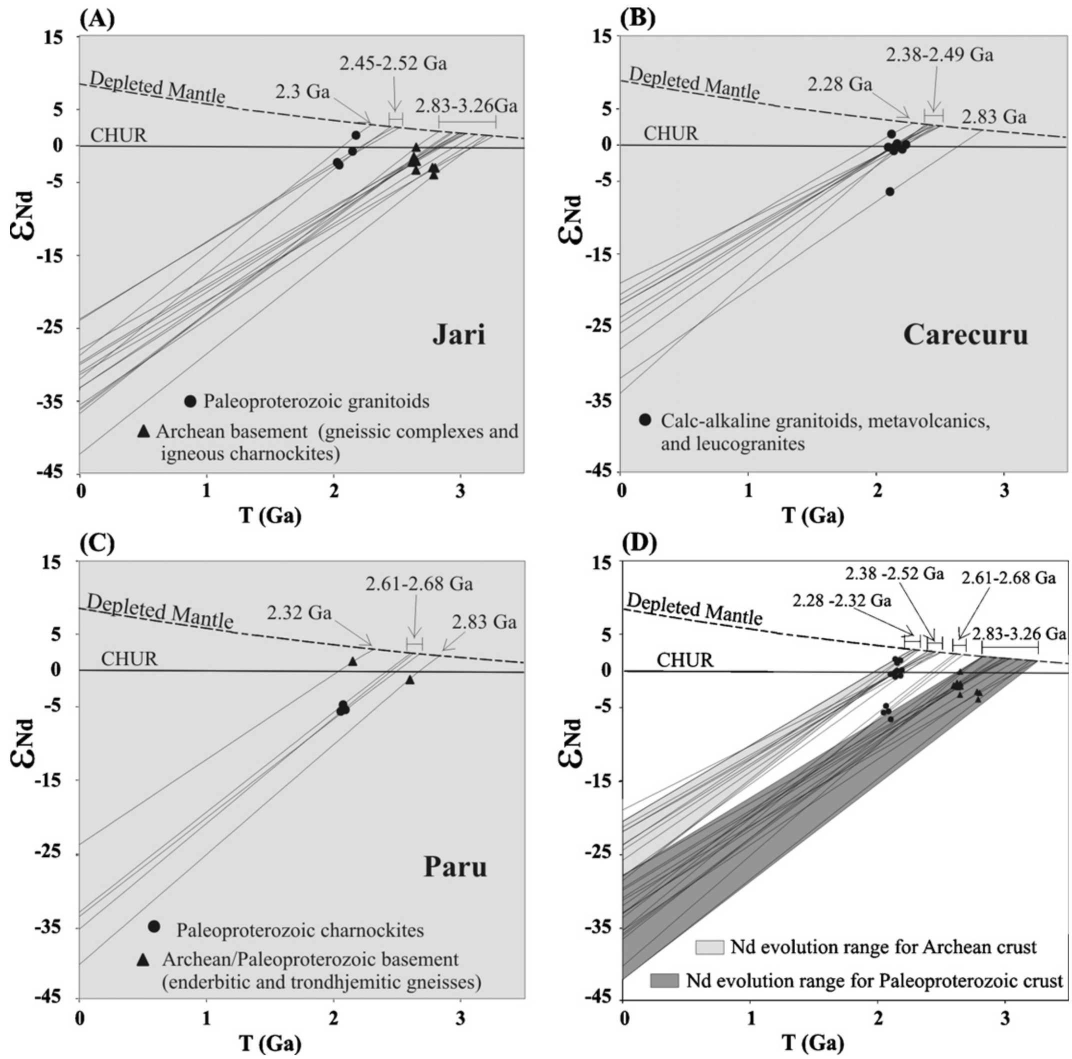

Fig. 5. Diagrams of Nd isotopic evolution for rocks from the Jari (A), Carecuru (B) and Paru (C) domains, and (D) Nd isotopic evolution for all analyzed samples. The Nd evolution ranges for Archean and Paleoproterozoic crust are based on data acquired in this work.

This coherent pattern supports the assumption that the interval between 3.26 and 2.83 Ga, which corresponds roughly to the Mesoarchean, can be considered as a protracted crust-forming episode, which is in agreement with the pattern of continental growth of the South America Platform during the Archean, based on Nd isotopic evolution (Cordani and Sato, 1999). The simultaneous determination of zircon ages and T_{DM} model ages allows the identification of two distinct geodynamic processes during Archean times in the Jari Domain. While juvenile crustal accretion is well documented since the end of the Paleoarchean and along the Mesoarchean, the lack of Neoarchean T_{DM} model ages and the negative ε_{Nd} values of the magmatism dated at about 2.80–2.79 Ga and between 2.66 and 2.60 Ga, indicate that the Neoarchean evolution was preferentially related to ensialic reworking of older Paleo-Mesoarchean crust.

The second group is constituted of Paleoproterozoic granitoids that yielded T_{DM} model ages mainly between 2.52 and 2.45 Ga and ε_{Nd} values between − 0.87 and − 2.51. One exception is the leucogranite (sample EK-89) that furnished T_{DM} and ε_{Nd} values of 2.30 Ga and +1.47, respectively.

A major Rhyacian crustal accretion event between 2.30 and 2.13 Ga has been recognized in Guiana Shield, from Guyana to northern Amapá region (Gruau et al., 1985; Lafrance et al., 1999; Nogueira et al., 2000; Voicu et al., 2000; Avelar, 2002; Roever et al., 2003). The Nd isotopic signature and the model age of the sample EK-89, which presents zircon age of 2185±44 Ma, indicate that its evolution is related to this regional period of crustal growth.

For the other samples of Paleoproterozoic granitoids, the Siderian T_{DM} ages of 2.52 to 2.45 Ga could indicate an older episode of crustal accretion at the Neoarchean–Paleoproterozoic transition. However, the existence of such an event could be a misinterpretation of the Nd isotopic results as no other geological and geochronological arguments support this hypothesis for the Guiana Shield, as well as in its African counterpart (West African Craton).

Firstly, no significant geological activity (i.e. magmatism or metamorphism) is known in the Guiana Shield and in the West African Craton during Siderian (Boher et al., 1992; Kouamelan et al., 1997; Doumbia et al., 1998; Gasquet et al., 2003;

Thiéblemont et al., 2004; Peucat et al., 2005). Even in global scale, Siderian is not recognized as an important period of crustal growth or of orogenic activities. In eastern Amazonian Craton, most of the geochronological records ranges between 3.3 Ga and 2.65 Ga and are lower than ca. 2.30 Ga. Only a few ages about 2.5 Ga have been registered, for instance, in the Carajás Province, where some small plutons of granitoids were dated around 2.60–2.50 Ga (Machado et al., 1991; Souza et al., 1995). In the Guiana Shield, the Neoarchean magmatic activity is well constrained from 2.80 Ga to 2.60 Ga but ages younger than 2.60 Ga have not yet been recorded (Avelar et al., 2003; Rosa-Costa et al., 2003; this work). In the whole eastern Amazonia, Siderian zircon ages of 2313±9 Ma, 2359±3 Ma and 2440±7 Ma have only been reported northward from the Carajás Province (Faraco et al., 2003; Macambira et al., 2004; Vasquez et al., 2005), but no Siderian Sm–Nd model ages have been reported for any rocks of that region.

Therefore, even if the hypothesis of Siderian crustal accretion episode at the Paleoproterozoic–Neoarchean transition, as advocated by Faraco et al. (2004), cannot be excluded in the Jari Domain, we prefer to consider these T_{DM} ages and negative values of ε_{Nd} in terms of mixing of two-components, with Paleoproterozoic juvenile mantle-derived magmas, contaminated by assimilation of Archean rocks or by interaction with magmas derived from Archean sialic sources, which are largely represented in the area. Such an hypothesis has been previously suggested by Avelar et al. (2003) to account for the late Neoarchean–Siderian T_{DM} ages of Paleoproterozoic granitoids from southeastern French Guiana. Siderian T_{DM} ages, slightly younger than those of rocks from the Jari Domain, have been also locally registered in 2.07–2.05 Ga old granulites and pegmatites from the Bakhuis mountains in northwestern Suriname (Roever et al., 2003). The T_{DM} ages of 2.40–2.35 Ga and ε_{Nd} values between +0.16 and −0.37 have been interpreted as recording an eo-Transamazonian crust-forming event with minor participation of reworked Archean crust.

3.2.2.2. Carecuru Domain. Eleven samples representing all stratigraphic units were analyzed in this domain. Paleoproterozoic crystallization ages were provided or estimated for all investigated samples. Fig. 5B highlights three distinct isotopic patterns of Nd isotopic evolution furnished by the studied samples. Rhyacian crustal accretion event is also recognized in this domain, indicated by the model age of 2.28 Ga and ε_{Nd} value of +1.63 furnished by the diorite LT-193. On the other hand, the syenogranite LT-207B, which has zircon age of 2098±2 Ma, exhibits a Nd T_{DM} age of 2.83 Ga, which is in agreement with the range of model ages furnished by Archean rocks of the Jari Domain. The strongly negative ε_{Nd} value of −6.61 indicates that the origin of this granite is related to partial melting of Archean crust. This T_{DM} model age of 2.83 Ga confirms the presence of Archean remnants in the Carecuru Domain, also indicated by the occurrence of inherited Archean zircons in Paleoproterozoic rocks, for instance in metarhyolite (sample LT-182C: Rosa-Costa et al., 2002a) and granodioritic gneiss (sample MV-65A: this work). However, conversely to what occurs in the Jari Domain, no Archean rocks are preserved in the Carecuru Domain.

The most remarkable pattern is provided by a group of rocks, including calc-alkaline granitoids, metavolcanics and granites, which gave T_{DM} model ages ranging from 2.49 to 2.38 Ga and slightly negatives ε_{Nd} values between −0.15 and −0.84, except in one sample (MV-65A), which gave a positive ε_{Nd} value of +0.22. Like the rocks of the Jari Domain, these Siderian model ages can be interpreted in terms of crust-forming age or as a result of mixing between Paleoproterozoic juvenile magmas and minor Archean continental component. In the current case, the latter assumption is reinforced by the occurrence of inherited zircons in the metarhyolite and granodioritic gneiss, which furnished Archean Pb–Pb ages significantly older than their respective model ages (sample LT-182C: T_{DM}=2.40 Ga and inherited zircon age of 2618±7 Ma—Rosa-Costa et al., 2002a; sample MV-65A: T_{DM}=2.45 Ga and inherited zircon age of 2784±6 Ma).

3.2.2.3. Paru Domain. In this domain, two gneisses were investigated, an Archean enderbitic gneiss of the Ananaí Complex and a Paleoproterozoic trondhjemitic gneiss enclosed within this complex, along with 3 charnockites that came from Igarapé Urucu Intrusive Suite.

The ε_{Nd} vs. time diagram (Fig. 5C) exhibits three clearly distinct patterns for the Nd isotopic evolution of the analyzed samples. The enderbitic gneiss MV-70D provided a Nd T_{DM} model age of 2.83 Ga and ε_{Nd} value of −1.6 that, combined with the age of the magmatic precursor at 2.60 Ga, previously acquired on zircon from the same sample (Rosa-Costa et al., 2003), indicate that this gneiss was produced by reworking of Mesoarchean continental crust during Neoarchean. However, the trondhjemitic gneiss LT-191A yielded a Nd T_{DM} age of 2.32 Ga and ε_{Nd} value of +1.17, characterizing the same eo-Transamazonian crustal accretion event that has been recognized in the other domains.

The 2.07–2.06 Ga charnockites furnished T_{DM} ages between 2.68 and 2.61 Ga, and negative ε_{Nd} values between −5.89 and −4.80. The strongly negative ε_{Nd} values indicate that the petrologic processes that originated these rocks include melting of an oldest crust during the Transamazonian orogenic event. This seems to be coherent if we consider that the formation of charnockites is related to the high grade event that affected the precursors of the surrounding Archean granulites of the Ananaí Complex. Nevertheless, if the charnockites are melting products of the enderbitic gneisses represented by sample MV-70D, which furnished a T_{DM} model age of 2.83 Ga, the Neoarchean model ages provided by the charnockites must be interpreted as mixed ages, produced by the participation of Archean and Paleoproterozoic components in the source of the charnockitic magma. A two-stage model for the Sm–Nd evolution of the source of charnockite with Sm–Nd fractionation during charnockitic magma formation would also account for T_{DM} ages (i.e. 2.68–2.61 Ga) younger than the T_{DM} age of the source rocks. However, the Sm–Nd ratios of both charnockites and enderbitic gneiss make this hypothesis unlikely. Alternatively, the T_{DM} ages of 2.68–2.61 Ga can correspond to the crust-formation time for the source of the charnockite, revealing a Neoarchean episode of crustal growth. Such an interpretation precludes the genetic relationship between charnockites and surrounding granulitic gneisses. The charnockitic magmas could be derived from younger (i.e. Neoarchean) and lower crustal segments accreted to the Mesoarchean segments by crustal underplating.

The diagram ε_{Nd} vs. time of Fig. 5D summarizes the Nd evolution patterns provided by all rocks analyzed from the different domains. The evolution ranges of the rocks are highlighted in the diagram that present four intervals of T_{DM} model ages. Two of these intervals undoubtedly define crustal growth episodes that vary, between 3.26 and 2.83 Ga and between 2.32 Ga and 2.28 Ga. The first one is characterized mainly in the Archean basement of the Jari Domain, whereas the latter is related to a regional-scale eo-Transamazonian crustal accretion event. The latter episode is recognized in all the domains but it represents a major event with significant production of crustal material only in the Carecuru Domain. The significance of the two other groups of Sm–Nd data, which present model age intervals of 2.52–2.38 Ga and 2.68–2.61 Ga is more questionable. Whether they represent two crust-forming episodes, respectively, during Neoarchean and Siderian times, or they reflect mixed ages between Transamazonian juvenile and Archean components is an issue that needs to be addressed, even if the latter hypothesis seems to be better sustained by the available geological and geochronological constraints.

4. Geodynamical implications

The new set of geochronological data, combined with those from previous geological and geochronological studies in the same area, demonstrate that the present-day configuration of the Jari, Carecuru and Paru Domains results from a complex evolution, constrained by multi-stage crustal growth and reworking events.

The continental crust of the Jari Domain has a long-lived evolution, which started at the end of the Paleoarchean and continued until Paleoproterozoic times (Fig. 6). Zircon geochronology reveals three phases of magmatic activity during Archean, i.e. at about 3.32 Ga, at the Meso-Neoarchean transition, ca. 2.80–2.79 Ga, and during the Neoarchean, between 2.65 and 2.60 Ga. Nd T_{DM} model ages reveal that the main period of crust formation occurred at the end of the Paleoarchean and during the whole Mesoarchean, in a protracted episode between 3.26 and 2.83 Ga. Conversely, the combination of zircon geochronology and Nd model age data characterizes the Neoarchean as a period of crustal reworking, without significant production of juvenile crust.

Considering the superficial distribution of the Archean rocks in the Jari Domain, represented by the gneissic-granulitic-migmatitic basement assemblage (Fig. 2), we can suppose that the continental crust was formed mainly at that time. The available data indicate that Paleoproterozoic rocks are almost restricted to plutons of granitoid and discrete supracrustal belts. During the Transamazonian orogenic cycle, the main geodynamical processes are related to reworking of older Archean crust, with minor juvenile accretion at about 2.3 Ga, associated to an early orogenic phase. Transamazonian magmatism consists of syn- to late-orogenic granitic pulses, which were dated at 2.22 Ga, 2.18 Ga, 2.15 Ga and 2.05 Ga to 2.03 Ga. Most of the isotopic Nd signature and T_{DM} model ages (between 2.52 and 2.45 Ga) indicates an origin by mixing of juvenile Paleoproterozoic magmas with Archean crustal components.

Conversely, the geodynamical evolution of the Carecuru Domain took place only in Paleoproterozoic times, mainly during the Rhyacian (Fig. 6). Eo-Transamazonian crustal accretion was recognized at about 2.28 Ga, in agreement with other Rhyacian crust forming ages registered in juvenile Transamazonian sectors of the Guiana Shield. Calc-alkaline magmatism is widespread, occurring apparently in two distinct pulses, at 2.19–2.18 Ga and at 2.15–2.14 Ga. Granitic magmatism was registered at 2.10 Ga, and can be envisaged as marking a stage of Paleoproterozoic crustal reworking in the Carecuru domain. Archean remnants are revealed by the model age of 2.83 Ga and by inherited zircon grains of some Paleoproterozoic rocks. However, systematic T_{DM} model ages between 2.50 and 2.38 Ga with ε_{Nd} slightly

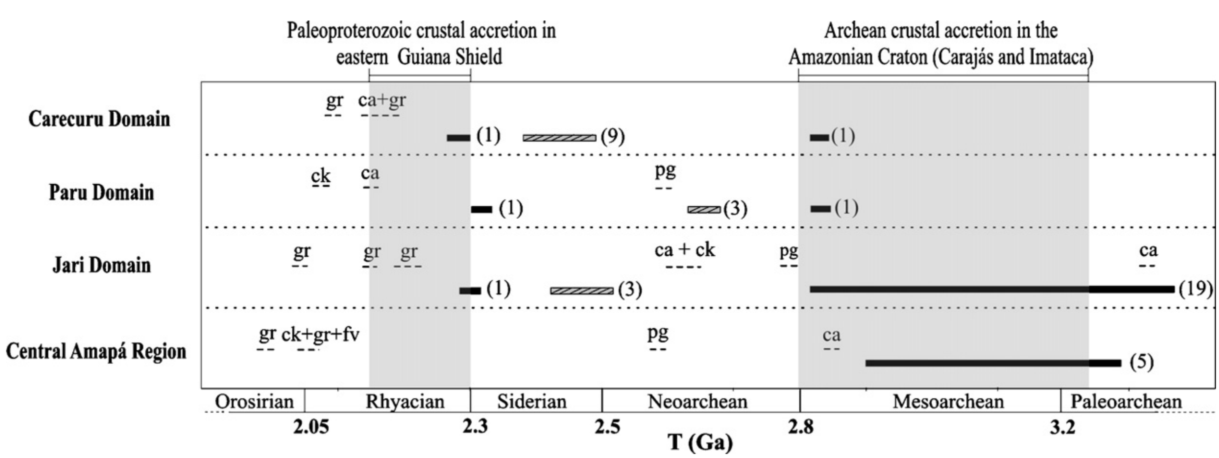

Fig. 6. Summary of the main crustal growth episodes and magmatic pulses vs. time, registered in the investigated domains and in central Amapá region. Magmatic pulses (dashed lines) and crustal growth episodes (black bars) based on zircon ages and T_{DM} model ages, respectively. Conventions: ca—calc-alkaline, gr – granitic, ck – charnockitic, pg – precursor granulitic, fv – felsic volcanic, hatched grey bars – mixed T_{DM} model ages, (*n*) number of dated samples. Source of data: Avelar (2002), Avelar et al. (2003), Barros et al. (2004), Borges et al. (2002), Cordani and Sato (1999), Gruau et al. (1985), Klein et al. (2003), Lafrance et al. (1999), Macambira and Lafon (1995), Nogueira et al. (2000), Pimentel et al. (2002, 2003), Ramö et al. (2002), Ricci et al. (2002), Roever et al. (2003), Rosa-Costa et al. (2002a, 2003), Sato and Tassinari (1997), Souza et al. (2001), Tassinari and Macambira (1999), Tassinari et al. (2001) and Voicu et al. (2000).

negative, preferentially interpreted as mixed ages, preclude any major participation of Archean components in the source of the Paleoproterozoic rocks.

The lithological association of the Carecuru Domain, i.e. large calc-alkaline plutons and mafic to intermediate volcanic rocks, is typical of subduction-related settings, being consistent with either a volcanic arc in oceanic environment or a magmatic arc at an active continental margin. However, the involvement of Archean crustal components shown by Nd isotopic signatures, added to the proximity of the adjacent Archean Jari Domain, strongly favors an origin in a magmatic arc setting.

Due to the scarcity of data, explanations concerning the tectonic significance of the Paru Domain in a Paleoproterozoic magmatic arc context are speculative. Some similarities can be recognized between the Paru and the Jari domains, which include T_{DM} model ages at about 2.83 Ga and Neoarchean magmatic events at about 2.6 Ga. However, besides contrasting geophysical and structural signatures between these domains (Rosa-Costa et al., 2002b), Paleoproterozoic calc-alkaline (2.15 Ga) and charnockitic (2.07 Ga) magmatism are known only in the former. At least two hypotheses can guide further investigations: (1) the Paru Domain represents a prolongation of the Jari Domain that was preserved in the roots of the magmatic arc; or (2) it is an allochthonous crustal fragment accreted to the magmatic arc during the Transamazonian orogenesis.

The next question to be addressed is the northeastern prolongation of the Archean continental crust. Several geochronological records of Archean rocks are known out of the limits of the investigated area, in the Cupixi region and vicinities (T_{DM} ages between 3.36 and 3.06 Ga—Sato and Tassinari, 1997; Pimentel et al., 2002; zircon age of 3321 ± 11 Ma—Klein et al., 2003), and more distant, in the Tartarugalzinho region, in the central portion of the Amapá state (T_{DM} ages between 3.29 and 2.9 Ga and zircon ages of ≈ 2.60 Ga—Lafon et al., 1998; Avelar et al., 2003). As such, the available evidence points to the existence of an expressive and, probably, continuous NW–SE structured Archean continental landmass extending from the Pará/Amapá border to the north of Tartarugalzinho region, here named Amapá Block (Fig. 7). The limits proposed for this block coincide with major tectonic structures, which are outlined by large Paleoproterozoic supracrustal belts. However, in the areas where geological and geochronological informations are not available, the limit must be regarded with caution, since it was inferred mainly on the basis of aerogeophysical imagery.

The major arguments that favor the nature of the Amapá Block as a continental landmass during the Transamazonian orogenic cycle are: (1) the dominantly Archean geochronological pattern; (2)

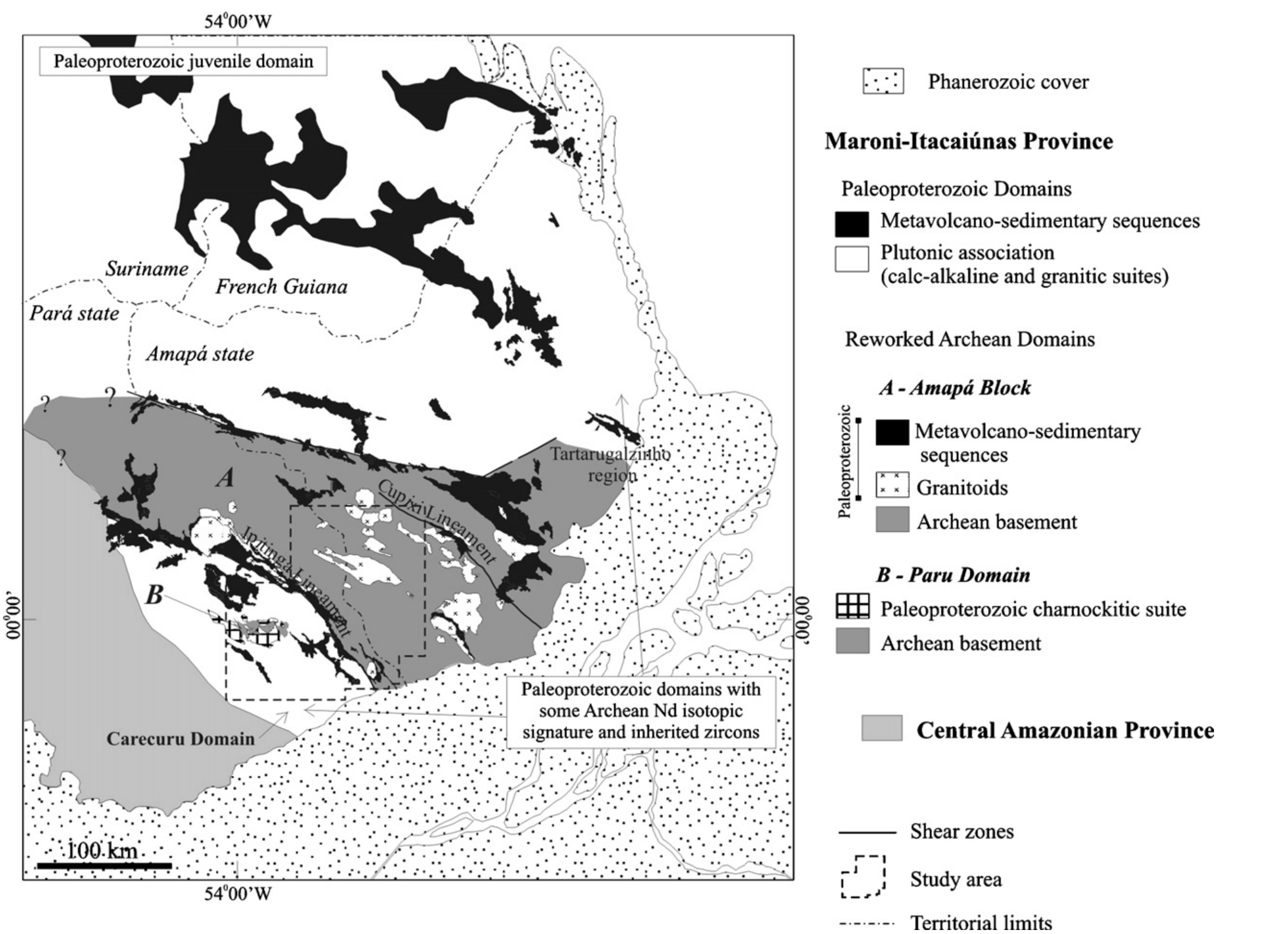

Fig. 7. Sketch map showing distinct geochronological/tectonic domains of the eastern Guiana Shield, including the Amapá Block defined in this study. Designation of the geochronological provinces according to Tassinari and Macambira (2004).

the lack of significant Transamazonian accretion and magmatism related to subduction processes; (3) the Nd isotopic signature which strongly indicates an origin of Paleoproterozoic granites by reworking of Archean crust.

Ricci et al. (2001) consider that the Jari Domain represents a tectonostratigraphic terrane, separated from the adjacent terranes by major NW–SE strike-slip shear zones: the Ipitinga Lineament, between the Carecuru and Jari terranes, and the Cupixi Lineament between the Jari and Cupixi terranes. The latter was originally named Cupixi-Tartarugal Grande Ancient Terrane, since it hosted the oldest dated rock in the southeastern Guiana Shield known until that time (2.85 Ga—Avelar et al., 2001). However, later geochronological studies have registered rocks older than 2.85 Ga in the Jari Domain (3.32 Ga—Klein et al., 2003; inherited zircon grains at about 3.24 Ga—this study). Therefore, a tectonic subdivision within the Archean block is still highly speculative, since there are not enough geological and geochronological arguments to support this hypothesis.

The recognition of an extended Archean landmass precludes previous statements that the Archean in the southeast of the Guiana Shield, was restricted to isolated remnants or inliers within Paleoproterozoic terrains (Tassinari and Macambira, 1999; Santos et al., 2000; Tassinari et al., 2000; Tassinari and Macambira, 2004). In addition, these Archean remnants were previously interpreted as a possible northward prolongation of the Archean Carajás range, strongly affected by the Transamazonian orogenic cycle, as discussed by Avelar et al. (2003).

In this work, we admit that the Amapá Block represents an independent continental landmass, rather than a northward prolongation of Carajás range, since the available geochronological data indicate distinct geodynamic evolution for these Archean segments. While a remarkable period of plutonic activity, between 2.80 and 2.60 Ga, took place during the Neoarchean in the Amapá Block, in the Carajás Province this phase corresponds to predominantly rift-related volcanism and sedimentary deposition (Gibbs et al., 1986; Wirth et al., 1986; Machado et al., 1991; Trendall et al., 1998), with emplacement of some plutons of granitoids in the north of the province (Machado et al., 1991; Souza et al., 1995; Avelar et al., 1999; Barros et al., 2004). In addition, in terms of lithologic content, tectonic features and metallogenic history, the differences are also outstanding. Furthermore, at north of the Carajás range, geochronological investigations showed widespread occurrence of Paleoproterozoic rocks (Macambira et al., 2001, 2004; Vasquez et al., 2005), in a magmatic arc environment (Macambira et al., 2001, 2004). This suggests the existence of a crustal segment extending from the north of the Carajás Province to the southern border of the Amapá Block, which presents a geochronological pattern dominantly Paleoproterozoic. This segment includes the Carecuru Domain, and is related to the development of a magmatic arc system during the Transamazonian orogenic cycle.

In the same way, at north of the Amapá Block, Avelar et al. (2003) characterized a transitional zone, between the Archean Tartarugalzinho region and the juvenile Paleoproterozoic domains of the French Guiana. In that zone, zircon ages defined Paleoproterozoic magmatic events between 2.19 and 2.09 Ga, but T_{DM} model ages, ranging from 2.75 to 2.39 Ga, indicate the existence of Archean components in the source of the Paleoproterozoic magmas. Some similarities can be outlined between the transitional zone described by Avelar et al. (2003) and the Carecuru Domain, for instance, calc-alkaline magmatism at about 2.19 Ga and the participation of Archean crust in the source of the Paleoproterozoic magmas. Moreover, in the northern portion of this transitional zone, Nogueira et al. (2000) dated tonalitic magmatism at 2.16 Ga and admitted that it is related to the development of a calc-alkaline magmatic arc.

Consequently, the Transamazonian orogenic cycle can be envisaged as a dominantly accretionary-type orogeny, responsible for the welding of several Archean continental landmasses (Carajás, Imataca Block, Amapá Block and also the Kénéma Man Domain in West Africa Craton) through arc systems (continental and oceanic), where reworking of continental crust and accretion of juvenile material played major roles. This major tectonic event resulted in the development of the extensive Paleoproterozoic belt of the northeast of the Amazonian Craton, which corresponds to the Maroni-Itacaiúnas Province or to the Transamazonic Province, according proposals of Tassinari and Macambira (2004) and Santos et al. (2000), respectively. As the major Archean blocks recognized within this belt, the Imataca Block and the here defined Amapá Block, are overprinted by the Transamazonian orogenesis, the proposal of Tassinari and Macambira (2004) is preferred since it is based on the age of the late orogenesis that affected the province. Nevertheless, the Amapá Block has to be incorporated in that model as an extensive Archean continental landmass instead of restricted Archean inliers.

Acknowledgements

The field work, sampling and petrographic study were performed during the mapping program (RENCA Project) developed by CPRM-Belém that started the new geological approach in the studied area. The expertise help with sample processing and zircon separation received from M.R. Soares (CPRM-Belém) and L.A. Costa e Silva (CPRM-Porto Alegre) is greatly appreciated. E. Oliveira, R. Florencio, R. Monteiro and especially M.A. Galarza are acknowledged for continuous technical assistance during the geochronological analyses at the Pará-Iso Laboratory, Belém. E. Klein (CPRM-Belém) is thanked for his helpful comments and suggestions. We are also grateful to J.J. Peucat and C.C.G. Tassinari for their expert and constructive reviews, which benefited substantially this article. This paper is a contribution to PRONEX/CNPq (Proj. 103/98-Proc. 66.2103/1998-0).

Appendix A. Description of dated samples

Mineral abbreviations: plagioclase—pl, quartz—qz, alkali feldspar—Kfs, biotite—bt, hornblende—hb, orthopyroxene—opx, clinopyroxene—cpx, garnet—grt, opaque minerals—opq, apatite—ap, zircon—zr, sphene—sph, monazite—mz, allanite—al, epidote—ep, sericite—sr, chlorite—chl, muscovite—ms.

Jari-Guaribas Complex: samples JM-60 (N00°09′57″/W52°37′30.09″), MV-27A (N00°45′04.01″/W53°11′16.01″) and MV-48 (N00°55′04.01″/W53°05′41.05″)—enderbitic to charnoenderbitic gneisses, grey and medium-grained. The mineralogical assemblage in equilibrium is defined by antiperthitic pl, qz, bt, mesoperthitic Kfs, with minor cpx, opx and opq. Hornblende occurs only in the gneiss MV-48. Accessories are ap and zr, besides mz in the sample MV-27A. These rocks present pervasive foliation and in the sample MV-48 the compositional banding is well defined. Microscopically, the texture is granoblastic (JM-60, MV-27A), with polygonal or interlobate contacts, or granolepidoblastic (MV-48). Mafic minerals are grouped in bands, with preferred orientation. Metamorphic retrogressions are chloritization of the bt, pyroxenes altered to bt or hb and pl to sr.

Baixo-Mapari Complex: sample MV-39 B (N00°46′01.01″/W53°05′32″)—pink, medium-grained granitic gneiss. The mineralogy is composed of mesoperthitic Kfs, qz, hb, bt, pl, opq, and accessories are ap and zr. It presents a well-defined banding, characterized microscopically by alternating granoblastic quartz-feldspatic and lepidoblastic mafic layers. Locally the pl is partially altered to sr.

Guianense Complex: samples LT-40 (N00°03′58.98″/W53°00′39.70″), LT-123A (S00°06′00.11″/W52°57′08.61″) and LT-126A (N00°03″16.70″/W53°00′56.29″)—medium-grained grey gneisses, classified in terms of igneous terminology, as tonalitic gneiss (LT-123A), granodioritic gneiss (LT-40) and mozogranitic gneiss (LT-126A). The mineralogy is pl, qz and Kfs, with variable amounts of bt. Accessories are ap, zr and al. The gneisses exhibit a well-defined banding, produced by alternating of centimeter-scale bt-rich and quartz-feldspar-rich layers. Microscopically, the texture is defined by interlaid granoblastic and lepidoblastic bands (LT-40, LT-126A) or is porphyroclastic (LT-123A).

Sample LT-11A (S00°14′07.30″/W52°45′36.91″)—a coarse-grained granodioritic augen gneiss, composed of pl, qz, bt, hb and Kfs. Accessories are sph, ap and zr. The texture is milonitic, defined by 1–3 cm long augens of Kfs or quartz-feldspatic aggregates, surrounded by strings of mafic minerals and medium-grained quartz-feldspatic long shaped aggregates. Metamorphic retrogressions in these gneisses are indicated by chloritization of the hb and bt, alteration of the bt to ms and sericitization of the pl.

Noucouru Intrusive Suite: samples JM-07 (S00°02′25.81″/W52°48′18.12″), LT-213 (N00°30′58.57″/W52°38″02.52″), LT-218 (N00°27′38.74″/W52°35′40.23″), MV-18A (N00°53′33″/W53°21′43.02″) and NR-39 (N00°25′42″/W52°31′49″)—they are medium- to coarse-grained rocks, rose, greenish or brownish, massive or weakly deformed, classified as mesoperthite-granites (NR-39, LT-213, LT-218), charnockite (MV-18A) and gr-charnoenderbite (JM-07). The mineralogy is composed of mesoperthitic Kfs, qz, antiperthitic pl, bt, hb, opx, cpx, grt, opq, ap, zr and al. Opx occurs in the samples JM-07 and MV-18A and cpx and gr only in the former. The texture can be inequigranular (LT-213, LT-218, MV-18A) with interlobate contacts, or porphyroclastic (JM-07), with medium-grained granuloblastic polygonal matrix.

Paru-Maratiá Complex: samples LT-196B (S00°09′26.70″/W53°47′03.23″), LT-202A (S00°21′58.51″/W53°43′07.79″), LT-206A (S00°28′37.79″/W53°37′25.10″) and MV-65A (N00°10′25.18″/W53°51′21.81″)—grey to pale grey and medium- to coarse-grained gneisses. The mineralogy is defined by pl, qz, Kfs, bt, hb, opq and grt. The hb occurs in the samples LT-196B and LT-202A, and the grt is present only in the sample MV-65A. The accessories are ap, zr and sph. In terms of igneous terminology, they are classified as dioritic (LT-196B), tonalitic (LT-202A) and graodioritic (LT-206A, MV-65A). The texture is inequigranular interlobate (LT-206A), with qz recrystallised and preferred orientation of the bt, or protomilonitic (LT-196A, LT-201, LT-202A, MV-65A), defined by porphyroclasts of pl, Kfs or hb, within a fine- to medium-grained recrystallised matrix, containing polycrystallines ribbons of qz and mafic anastomosed bands. Retrograde alterations are pl sericitized, hb altered to bt or chl and primary bt to chl.

Carecuru Intrusive Suite: samples LT-76 (S00°14′59.50″/W53°15′46″) and LT-193 (N00°06′36.65″/W53°15′45.94″)—they are diorites, grey to dark grey, medium- to coarse-grained. The sample LT-76 presents inequigranular hypidiomorphic to idiomorphic texture, and the sample LT-193 is weakly deformed, showing porphyroclastic texture. The mineralogy is composed of pl, hb, bt, qz, opq, sph, ap and zr.

Ananaí Complex: sample MV-70D (S00°02′31.69″/W53°47′32.31″)—leucoenderbitic gneiss, medium- to fine-grained, pale grey, where coexist in equilibrium pl, qz, opx, opq and cpx. Plagioclase is antiperthitic and coupled with qz defines about 90% of the rock. The pyroxenes are retrogressed to bt along cleavage planes. Accessories are ap and zr. The zr are small sub-rounded grains. In outcrop, this granulite is clearly foliated, and microscopically present granoblastic texture, with polygonal or interlobate contacts and pyroxenes showing a weak preferred orientation.

LT-191A (S00°01′31.31″/W53°50′03.41″)—pale grey and medium-grained trondhjemitic gneiss, defined by pl, qz, bt and opq. Quartz and pl represent more than 95% of the rock. The texture is inequigranular interlobate, with qz recrystallized in the boundaries and preferred orientation of the bt. Plagioclase is altered to white mica and bt to chl.

Igarapé Urucu Intrusive Suite: samples LT-185A (N00°04′30.69″/W53°48′26.60″), MV-68A (N00°06′30.20″/W53°49′05.62″) and MV-71A (N00°01′54.38″/W53°48′07.60″)—rose to pale brown, coarse grained igneous charnockites. The sample MV-71A presents porphyritic texture, defined by subhedral 0.5–2.0 cm long Kfs within a mediun-grained matrix. The samples LT-185A and MV-68A are more deformed and the texture is porphyroclastic. Alkali-feldspar and qz represent about 50% of the assemblage, coexisting with minor bt, pl, hb, opx, cpx and opq. The Kfs is strongly mesoperthitic. The opx and cpx are in equilibrium with other minerals or are replaced by hb and bt along fractures and cleavages planes. Accessory minerals are zr, ap, sph and al.

Granitoids: samples EK-89 (S00°20′05.36″/W52°52′13.69″), LT-17 (S00°03′47.50″/W52°57′58.91″), LT-114 (N00°07′11.49″/W53°13′22.60″), LT-177 (S00°08′47.80″/W53°16′42.81″), LT-201 (S00°20′10″/W53°45′35.21″), LT-207B (S00°29′29.62″/

W53°34′46.82″) and MV-07 (N00°35′37.98″/W53°09′07.99″)—they consist on pale rose to pale grey and medium- to coarse-grained leucogranites, weakly deformed or well foliated, composed of Kfs, qz, pl, with minor bt and opq, and the accessories are zr and ap. Based on quartz-feldspar ratios, they are classified as alkali feldspar-granite (MV-07), syenogranites (LT-17, LT-207B) and monzogranites (EK-89, LT-114, LT-177, LT-201). The granites EK-89, LT-177 and MV-07 present texture inequigranular hypidiomorphic, with qz variably recrystallised. The sample LT-17 contains bt and ms, besides grt, consisting in a typical two-mica granite. It presents milonitic texture, with porphyroclasts of Kfs in a matrix with quartz-feldspar recrystallized aggregates, polycrystalline ribbons of quartz and oriented strings of mica. The granite LT-114 is strongly striped, composed of alternating recrystallised quartz-feldspatic layers and quartz ribbons. In these rocks the pl is frequently altered to sr and ep and the bt is chloritized or transformed to ms. The granite LT-207B shows mylonitic texture.

Metavolcano-sedimentary sequences: *Fazendinha*—sample LT-61A (S00°11′16.20″/W53°09′16.51″)—grey and fine-grained massive rock. The composition is dacitic, defined by pl, qz, Kfs, bt, ms and opq. The texture is porphyritic, with euhedral pl within a fine grained matrix. *13 de Maio*—sample LT-182C (N00°26′11.83″/W53°10′40.07″)—white, fine-grained and foliated rock. The composition is dacitic to qz-andesitic (pl, qz, Kfs?, opq, mica). Microscopically, the texture is mylonitic, defined by oriented porphyroclasts of pl within a quartz-feldspatic fine matrix, with bands of opaque minerals and strings of white mica.

Parintins Intrusive Suite: sample JM-25 (N00°22′27.11″/W53°59′39.59″)—pale grey, mediun-grained and massive monzogranite, composed of qz, pl, Kfs, bt, opq, ap, zr and al. The texture is equigranular hypidiomorphic with interlobate contacts. Plagioclase is partially altered to white mica.

References

Ansdell, K.M., Kyser, T.K., 1993. Textural and chemical changes undergone by zircon during the Pb-evaporation technic. American Mineralogist 78, 1663–1673.

Avelar, V.G., 2002. Geocronologia Pb–Pb em zircão e Sm–Nd em rocha total da porção centro-norte do Estado do Amapá-Brasil: Implicações para a evolução geodinâmica do setor oriental do Escudo das Guianas, Tese de Doutorado, Universidade Federal do Pará, 213 p.

Avelar, V.G., Lafon, J.M., Correia Jr., F.C., Macambira, E.J.B., 1999. O magmatismo arqueano da região de Tucumã-Província Mineral de Carajás: novos dados geocronológicos. Revista Brasileira de Geociências 29, 453–460.

Avelar, V.G., Lafon, J.M., Delor, C., 2001. Geocronologia Pb–Pb em zircão e Sm–Nd em rocha total da porção centro-norte do Amapá. Implicações para a evolução geodinâmica do Escudo das Guianas. In: VII Simp. Geol. Amaz., Belém. CD ROM.

Avelar, V.G., Lafon, J.M., Delor, C., Guerrot, C., Lahondère, D., 2003. Archean crustal remnants in the easternmost part of the Guiana Shield: Pb–Pb and Sm–Nd geochronological evidence for Mesoarchean versus Neoarchean signatures. Géologie de la France 2–3–4, 83–100.

Barbarin, B., 1990. A review of the relationships between granitoid types, their origins and their geodynamic environments. Lithos 46, 605–626.

Barros, C.E.M., Macambira, M.J.B., Barbey, P., Scheller, T., 2004. Dados isotópicos Pb–Pb em zircão (evaporação) e Sm–Nd do Complexo Granítico Estrela, Província Mineral de Carajáas, Brasil: implicações petrológicas e tectônicas. Revista Brasileira de Geociências 34, 531–538.

Boher, M., Abouchami, W., Michard, A., Albarede, F., Arndt, N.T., 1992. Crustal growth in West Africa at 2.1 Ga. Journal of Geophysical Research 97, 345–369.

Borges, A.A.S, Lafon, J.M., Villas, R.N.N., 2002. Magmatismo Tardi-Transamazônico na Serra do Navio, região central do Ampá: evidências geocronológicas. XLI Cong. Bras. Geol. Anais, João Pessoa, p. 435.

Carvalho, J.M. de A., Rosa-Costa, L.T. da, Vasquez, M.L., Klein, E.L., Macambira, E.M.B., Vale, A.G., Ricci, P. dos S.F., 2001. Projeto Província Mineral da RENCA e Distrito Mineral do Ipitinga. CPRM-Serviço Geológico do Brasil, Belém, Mapa Geológico, escala 1:250.000.

Cordani, U.G., Sato, K., 1999. Crustal evolution of the South American Platform, based on Nd isotopic systematics on granitoid rocks. Episodes 22, 67–173.

Cordani, U.G., Tassinari, C.C.G., Teixeira, W., Basei, M.A.S., Kawashita, K., 1979. Evolução tectônica da Amazônia com base nos dados geocronológicos. II Cong. Geol. Chileno, Arica, Actas, vol. 4, pp. 137–148.

Cordani, U.G., Tassinari, C.C.G., Kawashita, K., 1984. A Serra dos Carajás como região limítrofe entre províncias tectônicas. Ciências da Terra 9, 6–11.

Delor, C., Lahondère, D., Egal, E., Lafon, J.M., Cocherie, A., Guerrot, C., Rossi, P., Trufert, C., Theveniaut, H., Phillips, D., Avelar, V.G., 2003a. Transamazonian crustal growth and reworking as revealed by the 1:500,000-scale geological map of French Guiana (2nd edition). Géologie de la France, 2–3–4, 5–57.

Delor, C., Roever, E.W.F. De, Lafon, J.M., Lahondère, D., Rossi, P., Cocherie, A., Guerrot, C., Potrel, A., 2003b. The Bakhuis ultrahigh-temperature granulite belt (Suriname): II. Implications for late Transamazonian crustal stretching in a revised Guiana Shield framework. Géologie de la France 2–3–4, 207–230.

DePaolo, D.J., 1981. Nd isotopic studies: some new perspectives on Earth structure and evolution. EOS 62, 137–145.

Doumbia, S., Pouclet, A., Kouamelan, A., Peucat, J.J., Vidal, M., Delor, C., 1998. Petrogenesis of juvenile-type Birimian (Paleoproterozoic) granitoids in Central Côte-d'Ivoire, West Africa: geochemistry and geochronology. Precambrian Research 87, 33–63.

Faraco, M.T.L , Vale, A.G., Santos, J.O.S., Luzardo, R., Ferreira, A.L., Oliveira, M.A., Marinho, P.A.C., 2003. Levantamento geológico na região norte do Bloco Carajás: notícias preliminares. In: VIII Simp. Geol. Amaz., Manaus. CD-ROM.

Faraco, M.T.L., Marinho, P.A.C., Vale, A.G., Moura, C.V., Macambira, M.J.B., 2004. Idades modelo Sm–Nd e idade ^{207}Pb–^{206}Pb em zircão no Distrito de Ipitinga, Reserva Nacional do Cobre e seus Associados-RENCA. XLII Cong. Bras. Geol., Araxá. CD-ROM.

Gasquet, D., Barbey, P., Adou, M., Paquette, J.L., 2003. Structure, Sr–Nd isotope geochemistry and zircon U–Pb geochronology of the granitoids of the Dabakala area (Côte d'Ivoire): evidence for a 2.3 Ga crustal growth event in the Paleoproterozoic of West Africa? Precambrian Research 127, 329–354.

Gaudette, H.E., Lafon, J.M., Macambira, M.J.B., Moura, C.A.V., Scheller, T., 1998. Comparison of single filament Pb evaporation/ionization zircon ages with conventional U–Pb results: examples from the Precambrian of Brazil. Journal of South American Earth Sciences 11, 351–363.

Gibbs, A.K., Wirth, K.R., Hirata, W.K., Olzewski, W.J., 1986. Age and composition of the Grão Pará Group volcanics, Serra dos Carajás. Revista Brasileira de Geociências 16, 201–211.

Gruau, G., Martin, H., Leveque, B., Capdevilla, R., 1985. Rb–Sr and Sm–Nd geochronology of Lower Proterozoic granite-greenstone terrains in French Guyane, South America. Precambrian Research 30, 63–80.

Howell, D.G., 1995. Principles of terrane analysis. New Application for Global Tectonics. Charpman and Hall. 245 pp.

João, X.S.J., Marinho, P.A.C., 1982. Catametamorfitos Arqueanos da região centro-leste do Território Federal do Amapá. I Simp. Geol. Amaz., Belém, vol. 2. Anais, pp. 207–228.

Karabinos, P., Gromet, L.P., 1993. Applications of single-grain zircon analysis to the detrital studies and age discrimination in igneous suites. Geochimica et Cosmochimica Acta 57, 4257–4267.

Klein, E.L., Rosa-Costa, L.T. da, Lafon, J.M., 2003. Magmatismo Paleoarqueano (3,32Ga) na região do Rio Cupixi, SE do Amapá, SE do Escudo das Guianas. In: VII Simp. Geol. Amaz., Manaus. CD ROM.

Klein, E.L., Moura, C.A., Pinheiro, B.L.S., 2005. Paleoproterozoic crustal evolution of the São Luís Craton, Brazil: evidence from zircon geochronology and Sm–Nd isotopes. Gondwana Research 8, 1–10.

Klötzli, U.S., 1999. Th/U zonation in zircon derived from evaporation analysis: a model and its implications. Chemical Geology 58, 325–333.

Kober, B., 1986. Whole-grain evaporation for $^{207}Pb/^{206}Pb$-age—investigations on single zircons using a double-filament thermal ion source. Contributions to Mineralogy and Petrology 93, 482–490.

Kober, B., 1987. Single zircon evaporation combined with Pb^{+} emitter-bedding for $^{207}Pb/^{206}Pb$-age investigations using thermal ion mass spectrometry, and implications to zirconology. Contributions to Mineralogy and Petrology 96, 63–71.

Kober, B., Pidgeon, R.T., Lippolt, H.J., 1989. Single-zircon dating by stepwise Pb-evaporation constraints the Archean history of detrital zircons from the Jack Hills, western Australia. Earth and Planetary Science Letters 91, 286–296.

Kouamelan, A.N., Delor, C., Peucat, J.-J., 1997. Geochronological evidence for reworking of Archean terrains during the Early Proterozoic (2.1 Ga) in the western Côte d'Ivoire (Man Rise-West Africa Craton). Precambrian Research 86, 177–199.

Kröner, A., Jaeckel, P., Brandl, G., Nemchin, A.A., Pidgeon, R.T., 1999. Single zircon ages for granitoid gneisses in the Central Zone of the Lompopo Belt, southern Africa and geodynamic significance. Precambrian Research 93, 299–337.

Lafon, J.M., Rossi, P., Delor, C., Avelar, V.G., Faraco, M.T.L., 1998. Novas testemunhas de relíquias arqueanas na crosta continental paleoproterozóica da Província Maroni-Itacaiúnas (Sudeste do Escudo das Guianas). XL Cong. Bras. Geol. Anais, Belo Horizonte, p. 64.

Lafon, J.M., Rossi, P., Delor, C., Barbosa, O.S., 2001. Granulitos tardi-Transamazônicos (2,06 Ga) na região norte do Estado do Amapá: o charnoquito de Calçoene. In:VII Simp. Geol. Amaz., Belém. CD ROM.

Lafrance, J., Bardoux, M., Voicu, G., Stevenson, R., Machado, N., 1999. Geological and metallogenic environments of gold deposits of the Guiana Shield: a comparative study between St. Élie (French Guiana) and Omai (Guyana). Exploration and Mining Geology 8, 117–135.

Lameyre, J., Bowden, P., 1982. Plutonic rock types series: discrimination of various granitoid series and related rocks. Journal of Volcanolgy and Geothermal Research 14, 169–196.

Ledru, P., Johan, V., Milési, J.P., Tegyey, M., 1994. Markers of the last stages of the Paleoproterozoic collision: evidence for a 2 Ga continent involving cicum-South Atlantic provinces. Precambrian Research 69, 169–191.

Lima, M.I.C., Oliveira, E.P., Tassinari, C.C.G., 1982. Cinturões granulíticos da porção setentrional do Craton Amazônico. I Simp. Geol. Amaz., vol. 1. Anais, Belém, pp. 147–162.

Ludwig, K.R., 2004, Users manual for ISOPLOT/EX a geochronological toolkit for Microsoft Excel (version 3).

Macambira, M.J.B., Lafon, J.M., 1995. Geocronologia da Província Mineral de Carajás: Síntese dos dados e novos desafios. Boletim do Museu Paraense Emilio Goeldi. Ciencias da Terra 7, 263–288.

Macambira, M.J.B., Barros, C.E.M., Silva, D.C.C., Santos, M.C.C., 2001. Novos dados geológicos e geocronológicos para a região ao norte da Província de Carajás, evidências para o estabelecimento do limite Arqueano-Paleoproterozóico no sudeste do Cráton Amazônico. In: VII Simp. Geol. Amaz., Belém. CD ROM.

Macambira, M.J.B., Silva, D.C., Vasquez, M.L., Barros, C.E.M., 2004. Investigação do limite Arqueano-Paleoproterozóico ao norte da Província de Crajás, Amazônia Oriental. In: XLII Congr. Bras. Geol., Araxá, CD ROM.

Machado, N., Lyndenmayer, Z., Krogh, T.E., Lindenmayer, D., 1991. U–Pb geochronology of Archean magmatism and basement reactivation in the Carajás area, Amazonian shield, Brazil. Precambrian Research 49, 329–354.

McReath, I., Faraco, M.T.L., 1997. Sm/Nd and Rb/Sr systems in part of the Vila Nova metamorphic suite, northern Brazil. I, South Amer. Symp. Isotop. Geol., Campos do Jordão, pp. 194–196. Extended abstracts.

Montalvão, R.M.G., Tassinari, C.C.G., 1984. Geocronologia pré-cambriana do Território Federal do Amapá (Brasil). II Simp. Geol. Amaz. Anaiz, Manaus, pp. 54–57.

Montgomery, C.W., 1979. Uranium–lead geochronology of the Archean Imataca Series, Venezuelan Guyana Shield. Contributions to Mineralogy and Petrology 69, 167–176.

Montgomery, C.W., Hurley, P.M., 1978. Total rock U–Pb and Rb–Sr systematics in the Imataca Series, Guyana Shield, Venezuela. Earth and Planetary Science Letters 39, 281–290.

Nogueira, S.A.A., Bettencourt, J.S., Tassinari, C.C.G., 2000. Geochronology of the Salamangone gold deposit host-rocks, Lourenço district, Amapá, Brazil. Revista Brasileira de Geociências 30, 261–264.

Norcross, C.E., Davis, D.W., Spooner, E.T.C., Rust, A., 2000. U–Pb and Pb–Pb age constrainsts on Paleoproterozoic magmatism, deformation and gold mineralization in the Omai area, Guyana Shield. Precambrian Research 102, 69–86.

Onstott, T.C., Hargraves, R.B., 1981. Proterozoic transcurrent tectonics: paleomagnetic evidence from Venezuela and Africa. Nature 289, 131–136.

Onstott, T.C., Hargraves, R.B., York, D., Hall, C.M., 1984. Constraints on the motions of South American and African Shields during the Proterozoic: I. $^{40}Ar/^{39}Ar$ and paleomagnetic correlations between Venezuela and Liberia. Geological Society of America Bulletin 95, 1045–1054.

Peucat, J.-J., Capdevila, R., Drareni, A., Mahdjoub, Y., Kahoui, M., 2005. The Eglab massif in the West African Craton (Algeria), an original segment of the Eburnean orogenic belt: petrology, geochemistry and geochronology. Precambrian Research 136, 309–352.

Pimentel, M.M., Ferreira Filho, C.F., Spier, C.A., 2002. Estudo Sm–Nd do Complexo Máfico-Ultramáfico Bacuri, Amapá: idade da intrusão, metamorfismo e natureza do magma original. Revista Brasileira de Geociências 32, 371–376.

Pimentel, M.M., Lindenmayer, Z.G., Laux, J.H., Armstrong, R., Araújo, J.C., 2003. Geochronology and Nd isotope geochemistry of the Gameleira Cu–Au deposit, Serra dos Carajás, Brazil: 1.8–1.7 hydrothermal alteration and mineralyzation. Journal of South American Earth Sciences 15, 803–813.

Ramö, O.T., Dall'agnol, R., Macamira, M.J.B., Leite, A.A.S., Oliveira, D.C., 2002. 1.88 Ga oxidized A-type granites of the Rio Maria region, eastern Amazonian Craton, Brazil: positively anorogenic! Journal of Geology 110, 603–610.

Ricci, P.S.F., Carvalho, J.M.A., Rosa-Costa, L.T., Klein, E.L., Vasquez, M.L., Vale, A.G., Macambira, E.M.B., Araújo, O.J.B., 2001. Geologia e recursos minerais do Projeto RENCA—Fase I. CPRM-Serviço Geológico do Brasil, Belém.

Ricci, P.S.F., Carvalho, J.M.A., Rosa-Costa, L.T, Lafon, J.M., 2002. Plúton charnoenderbítico Arqueano intrusivo nos ortognaisses granulíticos do Cinturão Jari-Terreno Arqueano expressivo do sudeste do Escudo das Guianas. XLI Cong. Bras. Geol. Anais, João Pessoa, p. 524.

Roever, E.W.F., Lafon, J.M., Delor, C., Cocherie, A., Rossi, P., Guerrot, C., Potrel, A., 2003. The Bakhuis ultrahigh-temperature granulite belt (Suriname): I. petrological and geochronological evidence for a counter-clockwise *P–T* path at 2.07–2.05 Ga. Géologie de la France 2–3–4, 175–206.

Rosa-Costa, L.T. da, Vasquez, M.L., Carvalho, J.M.A., Ricci, P.S.F., Lafon, J.M., 2001. Geocronologia preliminar do Arqueano e Paeoproterozóico do NW do Pará/SW do Amapá-Escudo das Guianas. In: VII Simp. Geol. Amaz., Belém. CD ROM.

Rosa-Costa, L.T. da, Macambira, E.M.B., Vasquez, M.L., Lafon, J.M., Ricci, P.S.F., 2002a. Idades de rochas metavulcânicas félsicas do sudeste do Escudo das Guianas. II Simp. sobre Vulcanismo e Ambientes Associados, BelémBoletim de Resumos e Roteiro de Excursão, p. 46.

Rosa-Costa, L.T. da, Vale, A.G., Silva, A.M., 2002b. Integração de dados aerogeofísicos e imagens de sensores remotos como ferrementa para o mapeamento geológico na Região Amazônica: o exemplo do Projeto Promin-RENCA. In: Klein, E.L., Vasquez, M.L., da Rosa-Costa, L.T. (Eds.), Contribuições à Geologia da Amazônia, vol. 3, pp. 227–243.

Rosa-Costa, L.T. da, Ricci, P.S.F., Lafon, J.M., Vasquez, M.L., Carvalho, J.M.A., Klein, E.L., Macambira, E.M.B., 2003. Geology and geochronology of Archean and Paleoproterozoic domains of the southeastern Amapá and northwestern Pará, Brazil—southeastern Guiana Shield. Géologie de la France 2–3–4, 101–120.

Rosa-Costa, L.T. da, Lafon, J.M., Cocherrie, A., Delor, C., submitted for publication. Electron microprobe U-Th-Pb monazite dating of the Transamazonian high-grade metamorphic overprint on Archean rocks from Amapá Block, southeastern Guiana Shield, northern Brazil. Journal of South American Earth Sciences.

Santos, J.O.S., Hartmann, L.A., Gaudette, H.E., Groves, D.I., Mcnaughton, N.J., Fletcher, I.R., 2000. A new understanding of the provinces of the Amazonian Craton based on integration of field mapping and U–Pb and Sm–Nd geochronology. Gondwana Research 3, 453–488.

Sato, K., Tassinari, C.C.G., 1997. Principais eventos de acreção continental no Cráton Amazônico baseados em idade-modelo Sm–Nd, calculada em evoluções de estágio único e estágio duplo. In: Costa, M.L.C., Angélica, R.S. (Eds.), Contribuições à Geologia da Amazônia, vol. 1, pp. 91–142.

Souza, S.R.B., Macambira, M.J.B., Horbe, M.A., 1995. Geochronological and isotopic evidences of the influence of the Paleopoterozoic Pojuca Granite on the Cu–Zn (Au–Mo–Ag) deposit, Carajás Province, Brazil. Symp. Rapakivi Granites and Related Rocks, Belém, p. 76. Abstracts.

Souza, Z.S., Potrel, A., Lafon, J.M., Althoff, F.J., Pimentel, M.M., Dall'agnol, R., Oliveira, C.G., 2001. Nd, Pb and Sr isotopes in the Identidade Belt, an Archean greenstone belt of Rio Maria region (Carajás Province, Brazil): implications for the geodynamic evolution of the Amazonian Craton. Precambrian Research 109, 293–315.

Stacey, J.S., Kramers, J.D., 1975. Approximation of terrestrial lead isotopic evolution by a two stage model. Earth and Planetary Science Letters 26, 207–221.

Tassinari, C.C.G., Macambira, M.J.B., 1999. Geochronological provinces of the Amazonian Craton. Episodes 22, 174–182.

Tassinari, C.C.G., Macambira, M.J.B., 2004. A evolução tectônica do Cráton Amazônico. In: Mantesso-Neto, V., Bartorelli, A., Carneiro, C.D.R., Brito Neves, B.B. (Eds.), Geologia do Continente Sul-Americano: Evolução da Obra de Fernando Flávio Marques de Almeida, pp. 471–485.

Tassinari, C.C.G., Bettencourt, J.S., Geraldes, M.C., Macambira, M.J.B., Lafon, J.M., 2000. The Amazonian Craton. In: Cordani, U.G., Milani, E.J., Filho, A.T., Campos, D.A. (Eds.), Tectonic Evolution of South America, pp. 41–95.

Tassinari, C.C.G., Teixeira, W., Nutman, A.P., Szabó, G.A., Mondin, M., Sato, K., 2001. Archean crustal evolution of the Imataca Complex, Amazonian Craton: Sm–Nd, Rb–Sr e U–Pb (SHRIMP) evidences. In: VII Simp. Geol. Amaz., Belém. CD ROM.

Tassinari, C.C.G., Munhá, J.M.V., Teixeira, W., Palácios, T., Nutman, A.P., Sousa, C.S., Santos, A.P., Calado, B.O., 2004. The Imataca Complex, NW Amazonian Craton, Venezuela: crustal evolution and integration of geochronological and petrological cooling histories. Episodes 27, 3–12.

Teixeira, W., Tassinari, C.C.G., Cordani, U.G., Kawashita, K., 1989. A review of the geochronology of the Amazonian Craton: tectonic implications. Precambrian Research 42, 213–227.

Thiéblemont, D., Goujou, J.C., Ega, E., Cocherie, A., Delor, C., Lafon, J.M., Fanning, C.M., 2004. Archean evolution of the Leo Rise and its Eburnean reworking. Journal of African Earth Sciences 39, 97–104.

Trendall, A.F., Basei, M.A.S., Laeter, J.R., Nelson, D.R., 1998. SHRIMP zircon U–Pb constraints on the age of the Carajás formation, Grão Pará group, Amazon Craton. Journal of South American Earth Sciences 11, 265–277.

Vanderhaeghe, O., Ledru, P., Thiéblemont, D., Egal, E., Cocherie, A., Tegyey, M., Milési, J.J., 1998. Contrasting mechanism of crustal growth Geodynamic evolution of the Paleoproterozoic granite-greenstone belts of French Guyana. Precambrian Research 92, 165–193.

Vasquez, M.L., Lafon, J.M., 2001. Magmatismo tipo A de 1,75Ga na porção oriental do Escudo das Guianas-Estados do Amapá e Pará, Brasil. In: VII Simp. Geol. Amaz., Belém. CD ROM.

Vasquez, M.L., Macambira, M.J.B., Galarza, M.A., 2005. Granitóides Transamazônicos na região Iriri-Xingu, Pará-novos dados geológicos e geocronológicos. In: Horbe, A.M.C., Souza, V.S. (Eds.), Contribuições à Geologia da Amazônia, vol. 5, pp. 16–31.

Voicu, G., Bardoux, M., Stevenson, R., Jébrak, M., 2000. Nd and Sr isotope study of hydrothermal scheelite and host rocks at Omai, Guiana Shield: implications for ore fluid source and flow path during the formation of orogenic gold deposits. Mineralium Deposita 35, 302–314.

Wirth, K.R., Gibbs, A.K., Olszewski, W.J., 1986. U–Pb ages of zircons from the Grão Pará Group and Serra dos Carajás Granite, Pará, Brazil. Revista Brasileira de Geociências 16, 195–200.

Zhao, G., Cawood, P.A., Simon, A.W., Sun, M., 2002. Review of global 2.1–1.8 Ga orogens: implications for a pre-Rodinia supercontinent. Earth-Science Reviews 59, 125–162.